The energetics and structure of nickel clusters: Size dependence

Charles L. Cleveland and Uzi Landman
School of Physics, Georgia Institute of Technology, Atlanta, Georgia 30332-0430

(Received 4 September 1990; accepted 11 February 1991)

The energetics of nickel clusters over a broad size range are explored within the context of the many-body potentials obtained via the embedded atom method. Unconstrained local minimum energy configurations are found for single crystal clusters consisting of various truncations of the cube or octahedron, with and without (110) faces, as well as some monotwinnings of these. We also examine multitwinned structures such as icosahedra and various truncations of the decahedron, such as those of Ino and Marks. These clusters range in size from 142 to over 5000 atoms. As in most such previous studies, such as those on Lennard-Jones systems, we find that icosahedral clusters are favored for the smallest cluster sizes and that Marks' decahedra are favored for intermediate sizes (all our atomic systems larger than about 2300 atoms). Of course very large clusters will be single crystal face-centered-cubic (fcc) polyhedra: the onset of optimally stable single-crystal nickel clusters is estimated to occur at 17 000 atoms. We find, via comparisons to results obtained via atomistic calculations, that simple macroscopic expressions using accurate surface, strain, and twinning energies can usefully predict energy differences between different structures even for clusters of much smaller size than expected. These expressions can be used to assess the relative energetic merits of various structural motifs and their dependence on cluster size.

I. INTRODUCTION

The structural, electronic, and chemical characteristics of materials depend on the state (phase) and degree (size) of aggregation. Clusters, i.e., finite aggregates of up to tens of thousands of atoms, exhibit unique physical and chemical properties and a systematic study of the dependence and evolution of these properties with size allows elucidation of the transition from the molecular to condensed matter regimes.[1-4] Such investigations have become possible over the last two decades due to the development and proliferation of methods of preparation and characterization of clusters of various elemental materials and their compounds, as well as in differing charge states.

A particularly complex and intriguing issue is the structure of clusters and the dependence of structure on size. Difficulties in investigating this question are found on both the experimental and theoretical fronts. On the experimental side, the problem is twofold. First, since cluster systems are larger than ordinary molecules, but too small to be dealt with as ordinary bulk materials, they are not well suited to exploration of their structure using the traditional approaches of spectroscopy and x-ray diffraction. As a result, structural studies using electron diffraction are the preferred method of investigation and have been applied with significant success in studies mainly of gas phase clusters of rare gases[5-8] and molecular clusters.[9,10] For metallic clusters, data obtained through electron diffraction experiments is scarce, but valuable information has been obtained via high-resolution electron microscopy for metal clusters from a few hundred to thousands of atoms condensed on substrates.[11-26] In addition, a scanning tunneling microscope probe has recently been used to examine silver and gold clusters supported on a graphite surface.[27] Furthermore, metallic clusters supported on graphite surfaces have also been investigated using extended x-ray-absorption fine-structure (EXAFS) and related x-ray techniques.[28-32] Analysis of this data is complicated, however, by the interaction between the deposited cluster and the substrate and the multitude of cluster sizes present on the surface.[32]

In the case of structural studies of gas-phase clusters, analysis of the electron diffraction data is complicated by the clusters' finite size: they do not fill all space and so need not possess translational symmetry. Consequently, the analysis relies to a large extent on comparisons between the measured diffraction patterns (i.e., diffraction functions which give the intensity of the scattered electron beam as a function of momentum transfer) with the results of model calculations which simulate the experimental data, using prescribed interatomic interactions and ambient conditions. The analysis of the gas phase data is further complicated by the dependence of the structural characteristics of the system on the generation process and ambient conditions. Furthermore, small clusters (below a few tens of atoms) may undergo a radical structural change by the addition of a single atom (or molecule), and for both small and large clusters, a distribution (equilibrium or nonequilibrium depending on the preparation conditions) of structural isomers may be found for a given cluster size.

The above considerations motivate systematic theoretical studies of the structure and energetics of clusters as well as of modes of cluster growth, phase changes, and isomerization. A principal objective of such structural studies is the determination of size boundaries of energetic stability for various structural forms and the question of the transition from behavior characteristic of a finite system to that of a bulk system with increasing cluster size. Ideally, we would seek answers to the above questions for all cluster sizes and

 0021-9606/91/117376-21$03.00

for a range of temperatures. However, the plethora of possible structures and the isomerizations between them make such studies rather prohibitive. Instead, as several researchers previously have done, we limit ourselves in this study to consideration of a number of structures whose selection is motivated by energetic and morphological considerations, as well as guided by accumulated past experience. As a further simplification, the energetic optimization of the structures is performed at zero temperature and thus neglects entropic effects. Nevertheless, such studies are relevant for developing understanding and establishing a conceptual framework which could guide a rational approach to these complex structural issues, as well as aiding in the analysis of experimental data. In addition, obtaining the structural (and underlying energetic) trends, via minimization of the clusters' energies using a conjugate gradient technique, permits us to assess critically the validity of formulas which we derive on the basis of macroscopic arguments for the energies of various structural motifs. Our results demonstrate the remarkable adequacy for many cluster types of such "macroscopic" expressions, provided the input energies (such as crystal plane dependent surface energies, twinning energies, and strain energies associated with particular deformations) are known.

The majority of experimental[5-10] and theoretical[8,33-45] investigations to date on the structure of clusters have been on rare-gas clusters produced in supersonic beams during gas expansion. In such experiments, clusters can obtain stable structures (for each cluster size) since they are formed at high temperatures and thus may anneal effectively.[46] Using electron diffraction data and analysis via molecular dynamics simulations employing Lennard-Jones (LJ) pair interactions, these studies have established the presence of icosahedral structures for small rare gas clusters (RGCs) containing 40–800 atoms. Much bigger argon clusters (10^4–10^5 atoms) exhibit a crystalline face-centered-cubic (fcc) structure containing twin boundaries[8,47] (which are detected by extra reflections in the diffraction patterns). However, the structural evolution of rare gas clusters in the intermediate regime is somewhat elusive.

All theoretical studies of the energetics and structure of RGCs employed pair interactions (mostly LJ potentials). The most complete study of these systems is the recent one by Raoult *et al.*[8] These authors conclude on the basis of a relaxation method,[48] and using LJ potentials, that for clusters with less than 1600 atoms, the most stable structures belong to the icosahedral sequence, while for larger clusters the decahedral sequence is energetically more stable. Additionally, they found that although monotwinned fcc models have a slightly lower energy than crystalline fcc polyhedra, they are not expected to become the structurally stable form for RGCs containing less than $\sim 10^5$ atoms.

Theoretical investigations of the energetics and structure of metal clusters are complicated by the complex nature of bonding and cohesion in metals. While for very small clusters (mainly of alkali metals and aluminum) rigorous quantum chemical calculations have provided valuable structural information,[49,50] for larger clusters one must resort to approximate descriptions of the interatomic interactions. Such atomistic studies employing various levels of approximation have been performed[51-55] for clusters containing up to ~ 100 atoms.

Another approach in the investigation of the structure of metal particles, which has been used for a rather long time,[22,56-61] is founded on macroscopic concepts rather than atomistic structural optimization. This approach is based on the Wulff construction[56,57] which determines the equilibrium macroscopic morphology of the crystallite (see Sec. III) and on the theory of elasticity which allows estimates of the elastic strain energy for a given structure.[58] The first systematic study employing the above principles was that of Ino[58] who calculated the free energy of multiply twinned particles and compared it to that of an fcc crystal of the same volume using as input to the calculation macroscopic quantities characteristic of the material, such as cohesive, surface, twin-boundary, and elastic strain energies. In addition, the adhesive energy of interaction between the metal particle and the substrate support was included. The sequence of structures obtained from Ino's calculations is as follows: for metal particles smaller than a critical value (~ 100 Å in diameter for gold), structures based on the icosahedron are the most stable. For larger clusters, the optimal structures are truncated octahedra (these are semiregular polyhedra of 14 faces, sometimes called tetrakaidecahedra, or TKDs). In addition, it was concluded that the decahedra, specifically those called Ino's decahedra (see Sec. IV), are not structurally preferred at any size.

A modified Wulff construction was introduced by Marks[19] to include twin boundaries. Motivated by experimental observations,[22] this modified construction allows for reentrant faces at the twin boundaries of the decahedron, thus decreasing its surface energy. Consequently, Marks predicts the evolution in cluster structure with increasing cluster size to progress from icosahedral to decahedral and finally to truncated octahedral structures. The energetics underlying the above progression results from a balance between the relatively lower surface energies of the fivefold symmetric structures and the elastic strain energies inherent in them. Since the total surface energy of a cluster varies roughly as its surface area while its total elastic strain energy varies roughly as its volume, the latter must increase more rapidly with the cluster's size. At a critical size, the decahedral sequence of clusters becomes energetically more favorable than the icosahedral sequence since it is characterized by a smaller strain energy. It should be noted, however, that numerical estimates[19] failed to show stability of the decahedral structures in the intermediate cluster size regime. In this context, we remark that application of the modified Wulff construction requires, as input, quantities which are often difficult (or impossible) to obtain from experiments (such as elastic strain energies, surface and twinning energies). In this paper, we show how to calculate these quantities for a given model of the interaction potentials.

Motivated by the above considerations and the increasing experimental efforts aimed at determinations of the structures of metal clusters and elucidation of correlations between the structure and physical and chemical properties, we embarked on a systematic study of the dependence of the

structure of metal clusters on cluster size. Our studies are based on unconstrained minimizations (relaxations) of the energies of a multitude of structural motifs, with the interatomic potentials described via the many-body embedded atom method (EAM)[62–64] parametrized for nickel.[65]

In our studies, both the macroscopic and microscopic, atomistic approaches are pursued, thus providing a test on the adequacy of the macroscopic concepts. We conclude that the macroscopic expressions which we develop, in conjunction with accurately calculated values for the characteristic energies as input, provide a reliable framework for structural analysis.

We find that in the small cluster size regime (less than 2300 atoms), icosahedral structures are energetically preferred, while for somewhat larger clusters, the decahedra are more stable. Furthermore, the optimal single crystal polyhedron does not become more favorable than the best Marks' decahedron of similar size for clusters smaller than $\sim 17\,000$ atoms.

In the next section, we briefly review the embedded atom method. In Sec. III, we describe the development of macroscopic expressions for the energetics of various structural forms, as well as provide details of methods for calculations of surface, strain, and twinning energies. Results obtained via atomistic energy minimization are presented in Sec. IV and compared to those derived from macroscopic estimates. Finally, we summarize our results in Sec. V.

II. INTERACTION POTENTIALS

As is well known, pair potentials are generally not adequate for a description of the energetics in metals due to the density dependence of the interactions which underlie the cohesion of these materials. Nevertheless, for simple metals (e.g., free-electron metals), formulations based on density-dependent expressions for the total energy[66–69] (employing effective Hamiltonians within the context of pseudopotential theory) have been used with some success. However, since the effective Hamiltonian formulations, based on second-order perturbation theory with respect to the electron ion interaction, are limited to free-electron (*sp*-bonded) metals, we have represented the energetics of the material under study (nickel) using the embedded atom method (EAM)[62–64] which has been applied recently with significant success in studies of various transition-metal systems.[62–65,70–72]

The EAM is a semiempirical method which provides a convenient framework for atomistic calculations for metallic systems. In this method, the dominant contribution to the energy of the metal is viewed as the energy of embedding an atom into the local electron density provided by the other atoms of the system, represented by an embedding-energy function F. This dominant contribution is supplemented by short-range, two-body interactions due to a core–core repulsion ϕ. The basic idea underlying this method is thus the same as that which motivated the development of the effective-medium theory,[73,74] and both find their roots in the density-functional theory.[75]

The cohesive energy $E_{\rm coh}$ of the metal is given in EAM by the ansatz

$$E_{\rm coh}=\sum_i \left\{ F_i\left[\sum_{j(\neq i)} \rho_j^a(R_{ij})\right]+\frac{1}{2}\sum_{j(\neq i)}\phi_{ij}(R_{ij})\right\}, \qquad (1)$$

where ρ^a is the spherically averaged atomic electron density, the function ϕ_{ij} depends only on the species of atoms i and j, and R_{ij} is the distance between atoms i and j located at $\mathbf{R}_i$ and $\mathbf{R}_j$. Thus the background density for each atom i is determined as the superposition of electronic densities from other atoms, evaluated at the nucleus of the ith atom. As seen from Eq. (1), the total cohesive energy of the material is expressed as a sum over all atoms in the system of atomic energy contributions. In the EAM, the functions F and ϕ are determined by choosing for them functional forms which meet certain general requirements and fitting parameters in these functions to a number of bulk equilibrium properties of the solid such as lattice constant, heat of sublimation, elastic constants, vacancy formation energy, etc. From the several parametrization procedures which have been suggested, we have chosen the one described recently by Adams *et al.*[65]

III. MACROSCOPIC CALCULATIONS

A. Single crystals

For a macroscopic single crystal cluster of a given size and shape which only has flat facets, it is simple to calculate the energy if we know the energy per atom in the bulk crystal and the surface energy (surface energy per unit area) for each type of crystal face that is exposed. The macroscopic character is invoked in the neglect of corrections to bulk energy other than surface energies, such as "edge" and "vertex" energies.

Alternatively, if we are given surface energies for all the (possibly) relevant types of facets, we can ask what shape will minimize the energy under the constraint that its volume remain constant. Wulff[56,57] has provided a simple construction that gives the answer. Proceed from the origin in any direction. This direction defines the normal to a crystal surface. At a distance from the origin numerically equal to the surface energy of that surface, erect a normal plane. Go back to the origin and repeat the process for all other directions which may point to facets on the cluster. The smallest volume containing the origin inside all erected planes is similar (in the geometrical sense) to the minimum energy shape for a cluster of given size. The construction is perfectly general and handles even unfaceted surfaces.

We will call the minimum energy shape for a material its Wulff polyhedron. Some researchers use this term to denote an Archimedian solid, the truncated octahedron, whose surface holds six square (100) faces and eight equilateral hexagonal (111) faces. While this shape is indeed the minimum energy fcc polyhedron for surface energies given by a simple bond-breaking calculation,[76] it at best only resembles the minimum energy polyhedra for any realistic materials except by coincidence, so such a usage seems somewhat misleading.

In order to apply such macroscopic methods, we need surface energies, and possibly bulk energies, for the material from which the cluster is made. These may be difficult to acquire experimentally. Often the best information available for surfaces is only an average surface energy, undifferentiat-

ed by crystal face. One of the problems in applying the macroscopic approach to small clusters is being unsure whether any deficiencies that may arise do so from the method's fundamental approximations or from poor values for material properties. Thus such methods are frequently applied only qualitatively. However, in cases such as ours where the atomic interactions are specified, the required energies are not difficult to obtain. This will permit us to test, in at least one case, how well the macroscopic approach works when applied to small clusters when the input energies are precisely known.

The crystaline bulk system may be described as consisting of a basis of N atoms (where N is on the order of several hundred) within a parallelapiped computational cell defined by three fundamental translation vectors which describe the periodicity of the cell (i.e., the periodic boundary conditions). Furthermore, these vectors are treated as dynamic variables on the same level as atomic coordinates.[77] In fact, the atomic coordinates are only described in terms of the prevailing periodicity of the bulk system. Consequently, if so desired, a uniform strain could be applied to the system by imposing suitable constraints on the three translation vectors that represent the corresponding periodicity of the system under the specified strain.

To determine the bulk energy per atom and the density for our material (at 0 K), it is sufficient to minimize the energy of the system by varying the vectors defining the unit cell,[77] which we accomplish by using the conjugate gradient method.[78] This provides us with the bulk (per atom) energy for our material and also determines the bulk density. Using the EAM potentials for nickel, the calculated bulk energy (per atom) is $\epsilon_B = -4.450\,008\,08$ eV and the volume per atom is 10.9163 Å^3.[79]

To determine the surface energy at 0 K for an unstrained surface, we remove a periodic boundary condition, creating two free surfaces,[80] while holding the computational cell fixed since it is determined by the bulk crystal. Subsequently, we relax the energy of the system by varying atomic coordinates using the conjugate gradient procedure. The surface energy is then simply the difference between our relaxed system's energy and that of the relaxed bulk system divided by twice the area of one of the newly exposed surfaces.

We have performed such calculations for the low Miller index surfaces [(100), (110), and (111)] which contribute to the Wulff polyhedron. In addition, we can also insert a single (111) twinning fault into a bulk system, and relax both the computational cell and atomic coordinates to obtain the twinning energy. The results of these calculations are shown in Table I. We remark that the atomic energies near the centers of the slabs were very close to the bulk energy given above, which serves as evidence that these slabs are bulklike in their middles. We also note that relaxation has very little effect on the surface energies in nickel, all of which turned out to be somewhat smaller than the experimental, facially averaged value[81] of 0.1485 eV/Å^2 (2.380 J m^{-2}) (however, the experimental value may be questioned; see Ref. 62 for a discussion).

Note that the twinning energy is negative. This suggests that the minimum energy crystal structure for these interactions might be hexagonal close packed (hcp) instead of fcc. If we construct an hcp bulk system and minimize its energy, we find that the energy per atom is lower than that of the fcc system by only 4.6×10^{-4} eV. This is of little if any consequence in the study presented here, since other energies are much more important for our clusters.

With these energies, we are in a position to construct the Wulff polyhedron for nickel. Using the zero temperature surface energies[82] for Lennard-Jones 6-12 interactions, we can also do the same for that material (see also Ref. 51 for a more inclusive exploration of faceting for this and other Mie potentials, and Morse potentials, neglecting relaxation). These results are compared in Fig. 1.

The Wulff polyhedron for nickel is markedly more similar to the truncated octahedron than the one for Lennard-Jonesium. We will see that the differences between these polyhedra for nickel and Lennard-Jonesium exactly parallel differences we will observe in comparing our results for microscopic nickel clusters with those of Raoult *et al.*[8] for Lennard-Jonesium.

More quantitatively, Table II compares the ratios among the (111), (100), and (110) surface energies for nickel, Lennard-Jonesium, and an ideal material whose Wulff polyhedron is exactly the truncated octahedron. Both nickel and Lennard-Jonesium crystallites prefer to have their (100) faces somewhat nearer to their centers than does the truncated octahedron (i.e., the ratio $\gamma_{100}/\gamma_{111}$ for these materials is smaller than $2/\sqrt{3}$), increasing the relative area of those faces. Both also have (110) facets which the truncated octahedron lacks, but in nickel that facet is very narrow (less than one nearest-neighbor distance in width for clusters up to about 15 000 atoms) and, unlike the Lennard-Jones case,[8] these will never end up being advantageous for clusters as small as the ones we will examine later on an atomistic scale.

Let us now calculate the energy $E_W(N)$ of a Wulff polyhedron containing N atoms. Since (110) facets do not occur on clusters as small as the atomistic ones we will treat later, we will omit these faces in this calculation. Let us use a unit of length u_N for our cluster such that the distance from the center of given Wulff cluster of N particles to a face with

TABLE I. Interfacial energies for unstrained nickel slabs.

Interface	Unrelaxed surface or twinning energy	Relaxed surface or twinning energy
(111) surface	0.094 74 eV Å^{-2}	0.094 675 8 eV Å^{-2}
(100) surface	0.103 41 eV Å^{-2}	0.103 406 8 eV Å^{-2}
(110) surface	0.112 44 eV Å^{-2}	0.112 341 2 eV Å^{-2}
(111) twinning plane		−0.000 088 3 eV Å^{-2}

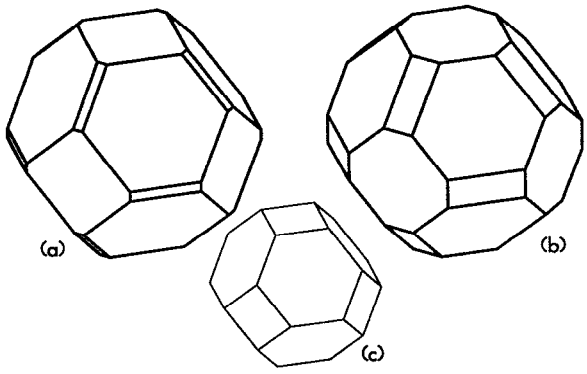

FIG. 1. The Wulff polyhedra for (a) nickel and (b) Lennard-Jonesium. Also shown for comparison is (c) the truncated octahedron.

surface energy γ is numerically equal to γu_N. For a given N, the surface energies thus determine the distances from the center of the cluster to its faces and specify the geometry of the polyhedron so that we may calculate the areas of its faces A_{111} and A_{100} and its volume V. For nickel, we find (with energy in units of eV and lengths in units of Å) that

$$E_W(N) = E_B(N) + 8\gamma_{111}A_{111} + 6\gamma_{100}A_{100} = \epsilon_B N + Cu_N^2, \quad (2)$$

where $C = 0.014\,970\,96$. Since the volume is given as

$$V = 8A_{111}\gamma_{111}u_N/3 + 6A_{100}\gamma_{100}u_N/3 = Cu_N^3/3 \quad (3)$$

and the volume per atom $V/N = 10.9163$, we can conclude that $u_N = 12.9812N^{1/3}$ and obtain for the Wulff polyhedron energy

$$E_W(N) = \epsilon_B N + 2.522\,79N^{2/3}. \quad (4)$$

B. Multitwinned particles

1. Icosahedra

An icosahedron (see Fig. 2) may be thought of as being composed of 20 distorted tetrahedral units all meeting at the center and each sharing three of its faces with neighboring units, leaving the last face to serve as one of the external icosahedral surface facets. Crystallographically, each face of the tetrahedron is an fcc (111) face and the plane of atoms which two neighboring tetrahedra share is a twinning plane, or put in other words, the stacking sequence in the direction normal to this plane is mirrored in it, ignoring the distortion of the tetrahedron.

Twenty perfect tetrahedral units, however, cannot be put together to make an icosahedron. If surface vertices of neighboring units are aligned, the units themselves will overlap at the icosahedron's center. To make a proper icosahedron, the tetrahedral units must be strained to make three of their sides, those meeting at the central vertex, about 5% shorter than the three which lay on the surface. This sort of strain is easy to accommodate within the Parrinello–Rahman description[77] employed for extended systems, in order to obtain the bulk and surface energies required for calculations of the cluster energies as described above.

For an unstrained system, each fundamental translation vector defining the periodically repeated cell could be taken as an integral multiple of one of the conventional primitive translation vectors for an fcc material [each pair of which defines a (111) plane]. This situation is represented in Fig. 3. In this figure, all the distances OA, OB, OC, AB, BC, and AC are equal. In order to apply icosahedral strain, we need only change the translation vector **c** so that the distances OC, AC, and BC become 4.894...% smaller than they were originally. [For further discussion of this sort of description of icosahedral (and decahedral) materials, see Ref. 59.] When minimizing the energy of a system with such a computational cell, the only parameter which we may vary is the volume. Doing so, and comparing with the corresponding result for the unstrained bulk, gives a strain energy (per atom) for uniform icosahedral strain of $\epsilon_\sigma^I = 0.032\,921\,95$ eV and a volume per atom of 11.0124 Å^3, slightly greater than that for an unstrained system.

It is instructive to use Ino's[58] expression for the energy due to a uniform icosahedral strain, with the elastic constants C_{11}, C_{12}, and C_{44} for our model of nickel, which are given in Ref. 65. The resulting value for the strain energy is 0.0349 eV. The agreement between this value and that obtained here by direct minimization indicates that for our interactions, nickel under uniform icosahedral strain is within the region of linear elastic behavior.

If we remove the periodic boundary condition associated with translation vector **c**, we create two surfaces like the $OADB$ plane in Fig. 3, which under the type of strain described above corresponds to the exposed face of a tetrahedral unit in an icosahedron. Fixing the shape of the computational cell as before and relaxing atomic coordinates yields a surface energy of 0.0795 eV/Å^2, nearly 16% lower than the unstrained value. (Without relaxation, the icosahedral surface energy would have been 0.0894 eV/Å^2.) Notice that unlike the case of the unstrained crystal (cf. Table I), surface relaxation has a significant effect here.

We may perform for the icosahedron an analogous calculation to that which gave us an expression [see Eq. (4)] for $E_W(N)$ for the Wulff polyhedron. If we ignore the twinning energy, which will be very small, we obtain (in units of eV)

TABLE II. Surface energy ratios for nickel and Lennard-Jonesium, along with those needed to produce a Wulff polyhedron that is exactly the truncated octahedron.

	Nickel	Truncated octahedron	Lennard-Jonesium
$\gamma_{100}/\gamma_{111}$	1.092	$2/\sqrt{3}(1.154...)$	1.054
$\gamma_{110}/\gamma_{111}$	1.187	$>\sqrt{3/2}(>1.224...)$	1.118

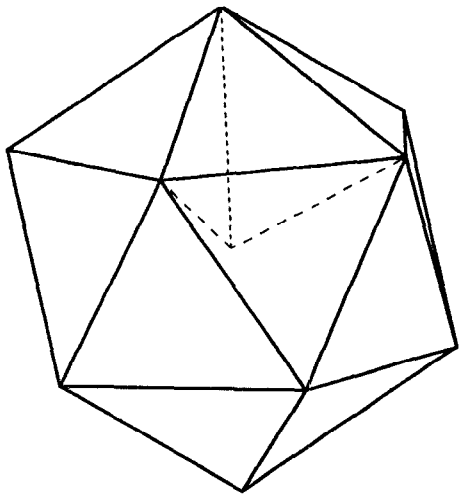

FIG. 2. The icosahedron and its relationship to the tetrahedral units of which it is composed.

$$E_I(N) = (\epsilon_B + \epsilon_\sigma^I)N + 2.027\,09N^{2/3}. \quad (5)$$

Comparing Eqs. (4) and (5), we can determine at what value of N the Wulff polyhedron becomes more energetically favorable than the icosahedron. We find the energies equal when $N = 3413$. In our microscopic atomistic calculations (see Sec. IV), we will find that the two energy curves for these two structural forms cross when $N = 3540$.

However, the remarkable agreement between the macroscopic estimate and that obtained from microscopic calculations is fortuitous in this case. If we compare the macroscopically calculated icosahedral energies with those obtained by atomistic minimizations of icosahedral clusters' energies, we find that the "real" clusters (i.e., those obtained via atomistic minimization) act as if their strain energy is substantially smaller than the value we have used here. In fact, relaxation of an icosahedral cluster from the "ideal" size and shape given by the macroscopic approach reduces the energy by a fraction almost an order of magnitude larger than that for decahedra and single crystals. In the icosahedron, strain can be relieved by letting the surface facets bow out in a nonplanar and nonuniform fashion at the expense of surface energy (see the discussion on icosahedra in Sec. IV). The two corrections nearly cancel for the range of cluster sizes where the energies of the icosahedra cross those of the Wulff polyhedra, so that the prediction made on the basis of the macroscopic calculation is deceptively good.

However, we will see that in systems under lower strain, such as the single crystals and the decahedra (whose uniform strain energy is 30 times smaller than the icosahedron's), the macroscopic calculations can indeed be used to produce quantitatively informative energy differences between cluster forms.

2. Decahedra

Figure 4 illustrates the kinds of "decahedra" we will be concerned with here. Of these, only the classic decahedron or pentagonal dipyramid actually has ten faces, the others being so called only because of their derivation from it.

The classic decahedron is, like the icosahedron, composed of slightly distorted tetrahedral units, five of which are joined at a common edge and each of which shares two of its (111) faces as twinning planes with neighboring units and contributes two other (111) faces to the surface of the decahedron. The faces on the classic decahedron are equilateral triangles. The principal advantage of the decahedron over the icosahedron lies in its lower strain energy. Part of this is due to the lower strain in the tetrahedral units of the classic decahedron and part is because in addition to being able to minimize strain energy by varying the volume of the units, we can also relax an additional degree of freedom corresponding to the length of the decahedron's central axis, shown as a dashed line in Fig. 4(a).

The relaxed classic decahedron shares with the icosahedron the advantage of only having (111) faces, but because of its much lower sphericity, its surface area is comparatively larger and energetically it is a poor competitor. Ino[58] suggested truncating the tetrahedral units as shown in Fig.

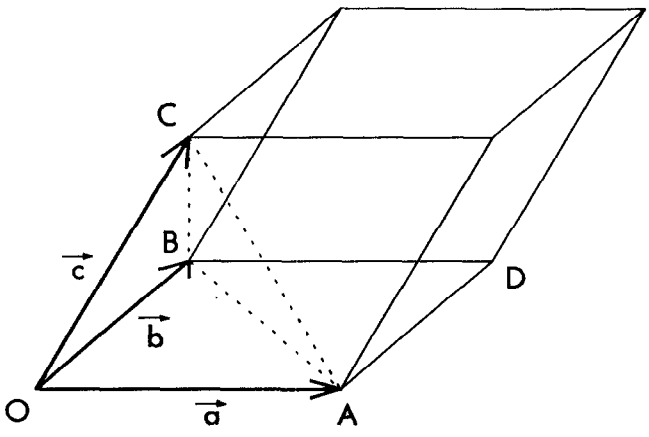

FIG. 3. An unstrained computational cell for fcc crystals. The three vectors **a**, **b**, and **c** are translations under whose repeated application the computational cell periodically fills all space.

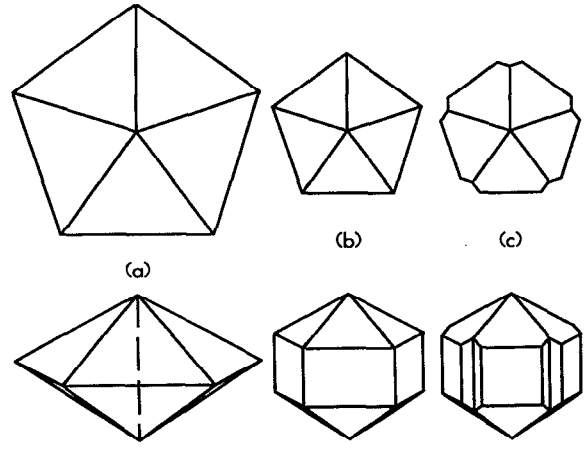

FIG. 4. (a) The classic decahedron, (b) an example of Ino's decahedron, and (c) an example of Marks' decahedron.

4(b), exposing (100) faces and making the structure more spherical. While this improves matters and also provides another parameter we may vary to minimize the energy of the polyhedron, Ino's decahedron is not the lowest energy structure for any known material, since as the polyhedra become larger and larger, the single crystals become more favorable than either the icosahedron or Ino's decahedron before the decahedron surpasses the icosahedron.

In an attempt to minimize the surface energy of the decahedron, however, we may give each of its single crystal tetrahedral units a surface like that of the single crystal Wulff polyhedron. This motivates Marks' modified Wulff construction[22] for decahedra, resulting in a nonconvex polyhedron like that in Fig. 4(c). In this construction, the distances from the origin to each surface plane are again taken to be simply proportional to that crystal plane's surface energy, and in addition, new "faces" are added in the directions corresponding to the decahedral unit's (111) twinning planes, ignoring strain. Since the interfacial energies of the twinning planes are very nearly zero, these planes almost pass through the origin and excise a wedge from the Wulff polyhedron that would otherwise have resulted. Thus the exposed surface of a unit in the decahedron, apart from being slightly stretched to fit, looks just like part of the surface of the Wulff polyhedron if the necessary strain does not significantly effect the surface energies. Figure 5 illustrates the relationship between the units of which Marks' decahedron is composed and the single crystal Wulff polyhedron.

For uniform decahedral strain, we may calculate the strain energy, and surface energies for the (100) face, the (111) "capping" face which touches the axis of the decahedron, and the (111) "notch" (or reentrant) face which makes Marks' decahedron nonconvex, as well as the twinning plane energy, by minimizing the energy of systems with two- or three-dimensional periodic boundary conditions, in a manner similar to our treatment of icosahedral strain. The details of such calculations are much more involved than the icosahedral case and are given in Appendix A. The resulting uniform strain energy per atom is $\epsilon_{\sigma}^{D} = 1.124\,426 \times 10^{-3}$ eV. The volume per atom is 10.9186 Å^3, only 0.02% more than that of the perfect single crystal. Table III displays the results for the surface and twinning energies, with the (110) surface omitted for simplicity [for nickel clusters in the range of sizes we concentrate on in this paper, (110) facets do not occur]. Notice that in contrast to the icosahedral case, relaxation effects for surface energies are small. Comparison with Table I shows that the change from the surface energies of an unstrained crystal are also small. The percentage change for the capping (111) face is -0.26%, that for the reentrant (111) face is -0.51%, and that for the (100) face is -0.48%. The twinning plane energy, although slightly larger and with the opposite sign than the unstrained case, is still negligible.

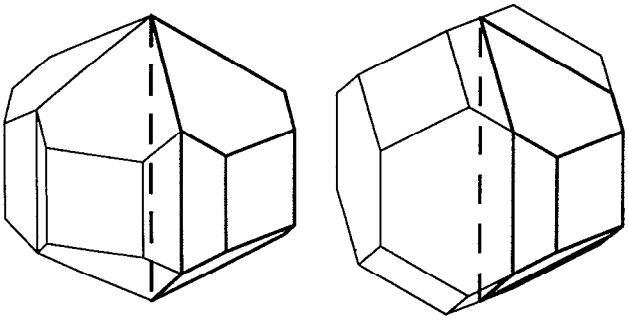

FIG. 5. The "tetrahedral" units of Marks' decahedron (left) and their relation to the Wulff polyhedron (right).

Given this information, we may seek an equation for the energy of the best Marks' decahedron, for a given volume or number of particles, just as we did for the Wulff polyhedra. This evaluation is described in Appendix B where we obtain for the optimal Marks' decahedron lacking (110) facets, the expression for the cluster's energy as a function of the number of atoms in it, $E_D(N)$; see Eq. (B1).

If we compare $E_D(N)$ with the Wulff polyhedron's energy $E_W(N)$ from Eq. (4), we can estimate that the single crystal will become more favorable than a Marks' decahedron when $N \approx 17\,000$. Clearly, clusters of this size may have (110) facets—in fact their width would be about one nearest-neighbor distance. Our neglect of them, however, occurs on both the Wulff polyhedron and the decahedron. They will effect the energies of both kinds of shapes similarly and that effect will be small since they are much smaller than the other faces. For nickel, at least, we do not feel that our estimation would be improved enough to warrant the increase in the complexity of the derivation given in Appendix B. As we will see from comparing energy differences between microscopic atomistic clusters of less than about 5000 atoms with corresponding macroscopic ones, the macroscopic treatment of clusters can be expected to be quantitatively quite good for clusters much smaller than 17 000 atoms.

IV. MICROSCOPIC CALCULATIONS

A. Single crystals and icosahedra

Prior to describing our microscopic, atomistic treatment, it is appropriate to discuss the nomenclature that we will use for different structural models of single crystal clusters. In general, it is not possible to fit an arbitrary number of atoms together in the shape of any given polyhedron, especially one like the Wulff polyhedron for nickel, the lengths of whose edges have nonsimple ratios. In addition, we examine clusters which depart from the ideal shape, not only because no clusters of microscopic dimensions exist for that precise shape, but also since we do not know *a priori* how reliable the macroscopic calculations are for such small clusters. Some of the cluster shapes which we examine already have conventional names, such as the cuboctahedron, the truncated octahedron, and the icosahedron. Others have no names outside the community of scientists studying small clusters and therefore need to be introduced for clarity.

The most extensive microscopic study to date is that of Raoult *et al.*[8] who studied the structure of Lennard-Jones microclusters and who have named many cluster models for the first time. Since there are no precedents, we will adopt much of their terminology in this paper.

All the fcc single crystal shapes which we will consider may be thought of as originating from a cube whose center is

TABLE III. Interfacial energies for nickel decahedra.

Interface	Unrelaxed surface or twinning energy	Relaxed surface or twinning energy
(111) surface (capping)	0.094 60 eV Å^{-2}	0.094 423 3 eV Å^{-2}
(111) surface (notch)	0.094 80 eV Å^{-2}	0.094 189 8 eV Å^{-2}
(100) surface	0.103 06 eV Å^{-2}	0.102 912 9 eV Å^{-2}
Twinning plane		0.000 166 3 eV Å^{-2}

the origin and whose eight vertices point in the (111) directions. A cube, along with some other Platonic and Archimedean solids, is shown in Fig. 6.

There are two fundamental families of such cubes—those with an atom at the origin and those with an fcc octahedral site there.[83] We will generally discuss only atom-centered clusters in this section, because the octahedral-site-centered clusters have little new to offer after the atom-centered ones have been examined. Apart from the decahedra, if the number of atoms in a single-crystal cluster is odd, the cluster is atom centered; if even, octahedral site centered.

Other polyhedra can be produced by "shaving off" layers of atoms corresponding to crystal planes we want to expose on the surface. When shaving off any face of atoms, we also remove all other similar ones, since we want to keep the shapes we consider as symmetric, and therefore as small in number, as possible. Repeatedly shaving (111) faces from a cube allows us to successively produce, at least approximately, a sequence of shapes like the Archimedean solids in Fig. 6. It also enables us to produce many other intermediate shapes as well. However, we cannot produce clusters of arbitrary shape, as we could macroscopically, since atoms must be removed as discrete units.

This aspect of atomicity is revealed explicitly in the way the choice of a particular geometric shape for a cluster restricts the number of atoms which it can contain. If we want to construct an icosahedron or cuboctahedron, we must use a number of atoms in the set {13, 55, 147, 309, 561, ...}, or to construct a truncated octahedron, we must choose from {38, 201, 1289, 4033, ...}, etc.

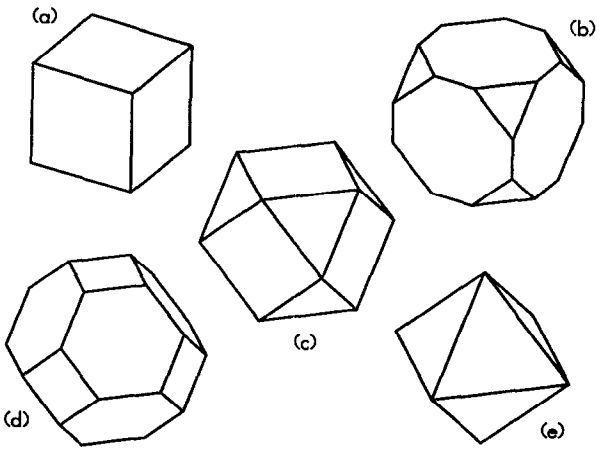

FIG. 6. A sequence of Platonic and Archimedian solids demonstrating the duality of the octahedron and the cube. Shown are (a) the cube; (b) the truncated cube; (c) the cuboctahedron; (d) the truncated octahedron; and (e) the octahedron.

This poses the question of which models we should consider? The truncated octahedron [Fig. 6(d)] is an obvious choice since of all the named shapes, it is closest to the Wulff polyhedron. We also consider local variations from this shape since it occurs sparsely and we want to examine similar shapes to fill the gaps in cluster size, as well as explore its local neighborhood in configuration space. Many of the models which we have considered are less than encouraging. In this paper, we concentrate on the more energetically favorable models and *a posteriori* explain the principles that might have led us to such models from the outset.

Let us construct our clusters from cuboctahedra [Fig. 6(c)] which have the convenient property that removing one atomic layer from each of its faces produces the next smaller cuboctahedron. (A similar observation holds for the icosahedra.) This causes the difference in the number of atoms between a cuboctahedron and the next one in size to be as small as possible. Taking the sequence of cuboctahedra,[84] we find that only for every fourth one can a truncated octahedron be produced by shaving off (111) planes of atoms. Nevertheless, Raoult *et al.*[8] have defined a sequence of clusters (named "model C") which closely resemble truncated octahedra and which can be made from every cuboctahedron. Accordingly, a cluster belongs to model C if its (111) faces are just further from the center than would be the case for the truncated octahedron and consequently are slightly smaller in comparison with the (100) faces. In this context, we remark that the Wulff polyhedron also has its (111) faces slightly further from its center than the truncated octahedron does. For any cuboctahedron, we have merely to shave off (111) planes until we come to the last one further from the origin than the ideal truncated octahedral distance. Thus we have four model C clusters for every truncated octahedron.[85]

Another sequence of clusters may be obtained by exposing (110) facets. Given any model C cluster, we can simply strip off the line of atoms at the edge where two (111) faces meet. This produces a small (110) face consisting of two parallel lines of atoms. Following Raoult *et al.*, we call these HKI clusters.[86]

The last sequence of single-crystal clusters which we consider are cuboctahedra. Many previous researchers have studied them, even though the shape is not very optimal,

because of the special relationship, alluded to earlier, that the cubocthedron has with the icosahedron. Not only do the two sequences contain clusters with the same numbers of atoms, but any cuboctahedral cluster can convert to an icosahedral one, and vice versa, by means of a simple twinning transformation.[87] Thus the competition between icosahedra and cuboctahedra is more direct and physical than that involving other single-crystal clusters, which generally cannot convert to other high symmetry clusters without gaining or losing atoms or at least undergoing substantial atomic rearrangement.

Finally, we will also include in our microscopic calculations the icosahedra, which are expected to be energetically optimal for the smallest clusters, and since we wish to investigate as a function of cluster size the transition from icosahedra to other structural forms, such as single crystals and cuboctahedra.

In Table IV some of the geometric properties of these clusters are collected. Here and elsewhere, m denotes the number of atoms on an edge joining a (111) face and a (100) face; n denotes the number of atoms on an edge between a (111) face and any non-(100) face—either (111) or (110) for our clusters. The number of atoms on an edge between a (100) face and a (110) face on an HKI cluster is always two.

First we will plot vs $N^{1/3}$ the energies (obtained by energy minimization using the EAM potentials) of these clusters less the bulk energy of the same number of atoms $E_B(N) = \epsilon_B N$ divided by $N^{2/3}$. Using macroscopic considerations as a guide, we expect that the total energy of a given cluster shape, with N atoms and surface area S, could be expressed in the form[58]

$$E(N) = \epsilon_B N + \epsilon_\sigma N + \epsilon_\gamma S, \tag{6}$$

where ϵ_B is the bulk energy per atom, ϵ_σ is the uniform strain energy per atom (zero for the single-crystal clusters), and ϵ_γ is an average surface energy per unit area for that cluster shape. Denoting by α a geometric factor suitable for that shape, we may write

$$[E(N) - \epsilon_B N]/N^{2/3} \approx \epsilon_\sigma N^{1/3} + \alpha\epsilon_\gamma. \tag{7}$$

Equation (7) is an approximate equality because quite large clusters may be necessary before the surface area can be well approximated by $\alpha N^{2/3}$ for a given cluster shape.

Thus a simple macroscopic approach would lead us to expect that plotting the energies of microscopic single-crystal clusters in this way will produce horizontal lines ranked according to how well they minimize surface energy, while the icosahedral curve will be a straight line with a positive slope caused by its internal strain.

In the upper panel of Fig. 7, we display the results of energy minimization for microscopic single-crystal clusters and the above expectations are born out. We also find that icosahedral clusters are most favorable for clusters containing less than 3540 atoms, at which point the truncated octahedra and model C clusters are very competitive with each other, as expected since their shapes bracket that of the Wulff polyhedron. As expected, we also find the (110) faceting of HKI clusters to be energetically unfavorable for smaller clusters and to become more attractive as cluster sizes increase, although we do not explore clusters large enough for it to become the optimal structural form. The cuboctahedron does not compete at all with the other clusters in this size range. However, extrapolation[88] of the cuboctahedral and icosahedral energies enables us to estimate that the cuboctahedrals are favored over the icosahedrals for clusters larger than about 14 000 atoms.

At this point we wish to compare the results obtained via the atomistic energy minimization with those of macroscopic calculations. To perform macroscopic calculations for an unrelaxed atomic cluster, we must be able to associate a polyhedron with it; i.e., we must take the cluster and find its set of surface planes. This defines the polyhedron and allows us to calculate its volume and various surface areas, which are used in a macroscopic calculation of the cluster's energy. We note that since we are dealing with rather small, atomic clus-

TABLE IV. Single crystal atom-centered clusters and icosahedra: number of atoms N, number of atoms on an edge between a (111) and a (100) face m, number of atoms on an edge between a (111) face and a non-(100) face n. Each truncated octahedron can be produced from the cuboctahedron in the same row by removing one or more sets of eight (111) planes, and if one fewer set of (111) planes is removed from each truncated octahedron, the model C cluster in the same row is produced.

Icosahedra/cuboctahedra[a]			Truncated octahedra			Model C			HKI		
N	m	n	N	m	n	N	m	n	N	m	n
147	0/4	4/1									
309	0/5	5/1	201	3	3						
561	0/6	6/1				405	4	3	369	2	4
923	0/7	7/1				711	5	3	675	3	4
1415	0/8	8/1				1139	6	3	1103	4	4
2057	0/9	9/1	1289	5	5	1709	7	3	1673	5	4
2869	0/10	10/1				1925	6	5	1865	4	6
3871	0/11	11/1				2735	7	5	2675	5	6
5083	0/12	12/1				3739	8	5	3679	6	6
6525[b]	0/13	13/1	4033	7	7	4957	9	5	4897	7	6
						5341	8	7	5257	6	8

[a] For m and n, the left-hand value is for icosahedra; the right is for cuboctahedra.
[b] Not studied here.

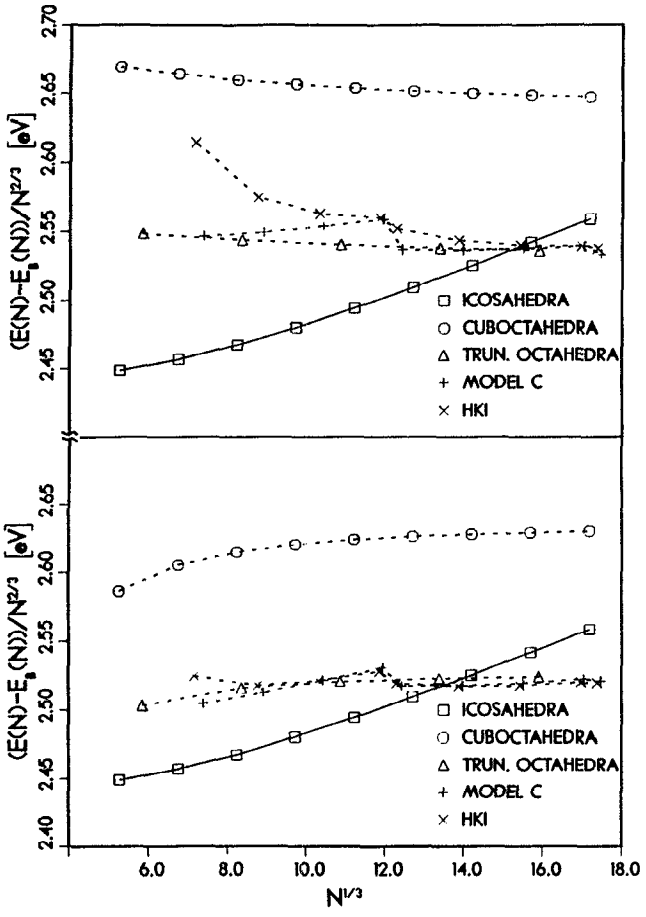

FIG. 7. In the upper panel of this figure, the minimized energies of microscopic single clusters are represented relative to the bulk, together with those of the icosahedra. In the lower panel, also relative to the bulk, are shown the energies resulting from macroscopic calculations for unrelaxed versions of the same clusters, along with the same icosahedral curve. In these macroscopic calculations, surface planes were taken to fall between atomic layers.

ters, it may make a substantial difference where we define those surface planes to fall. We might choose for one to cut through the atoms in the surface layer of its facet. Alternatively, we might choose for the surface plane to fall outside that plane by a distance equal to one-half the layer spacing for that crystal face. Each choice produces a different energy for every cluster we examine.

First, let us take a surface plane to lie above the surface atoms by one-half a layer spacing. Results of macroscopic calculations with this convention are shown in the lower panel of Fig. 7. The overall energies are are in adequate agreement with the corresponding microscopic ones, shown in the upper panel of Fig. 7, with the scaled energy differences in the figure too low by 0.03 eV for large clusters and worse for smaller ones. However, the relative ordering of the clusters in energy, particularly the truncated octahedron, model C, and HKI clusters, is poorly articulated and frequently wrong, even for larger ones.

Let us explore a different convention for positioning the surface planes in the macroscopic calculation and move these planes so that they pass through the cluster's surface atoms. If we were to plot the results in the usual way, we would initially be discouraged. All the single crystal clusters would have scaled energy differences substantially lower than *any* of the icosahedra, and for smaller clusters the deficiency would be much worse. However, upon closer examination, we observed that the relative ordering in energy of the clusters of similar size had been remarkably improved.

Results in which the energetics of various structural models are compared may be presented in various ways. In particular, we may use as our reference not $\epsilon_B N$, but the energies of the members of a standard reference family of clusters, such as the cuboctahedra, somewhat as van de Waal[40] does. The advantage of this approach over using the bulk energy as reference is that it subtracts cluster surface energies as well. While this is unimportant when presenting energies obtained via atomistic minimization, it is advantageous when displaying energies from macroscopic calculations for small clusters, since such a subtraction can largely correct for systematic errors, such as may be connected with the positioning of the surface planes. We will use the cuboctahedron as our reference cluster since it has no strain energy, it occurs at frequent intervals for better interpolation, and it will not be greatly missed from the figures since it is such a poor competitor.

Results obtained by atomistic energy minimization and via macroscopic calculations which take surface planes to pass through surface atoms are shown in Fig. 8. At the top, the microscopic results, using an interpolation[88] formula based on microscopic cuboctahedra are displayed. At the bottom, we show the results for macroscopic single-crystal polyhedra, using an interpolation formula based on macroscopic cuboctahedra. The icosahedral curve in both figures is the one obtained from our microscopic calculations since the macroscopic approach fails to provide an accurate estimate for this structure, as discussed in Sec. III. The overall agreement between the results obtained by the two approaches is remarkable. Note, however, the overestimation of the energies of the HKI clusters by the macroscopic calculations. Nevertheless, this discrepancy decreases as clusters become larger and the microscopic HKI clusters become more competitive energetically.

The use of cuboctahedral reference energies instead of bulk ones does not affect the relative energetic ordering of clusters of similar size, regardless of which convention is employed for positioning the surface planes with respect to atomic ones. The advantage of using cuboctahedral reference energies lies in being able to change the conventional location of the surface planes in order to improve the relative energetic ordering of clusters of similar size, since only clusters of similar size can energetically compete with one another.[89]

B. Icosahedra

There is substantial interest in the characteristics of relaxed icosahedral clusters. As we pointed out in Sec. III, systems under uniform icosahedral strain have a relatively large strain energy. Nonetheless, microscopically relaxed icosahedral clusters are energetically favored over other types even for clusters of several thousand atoms. It is worthwhile to examine the nature of the relaxation of icosahedral

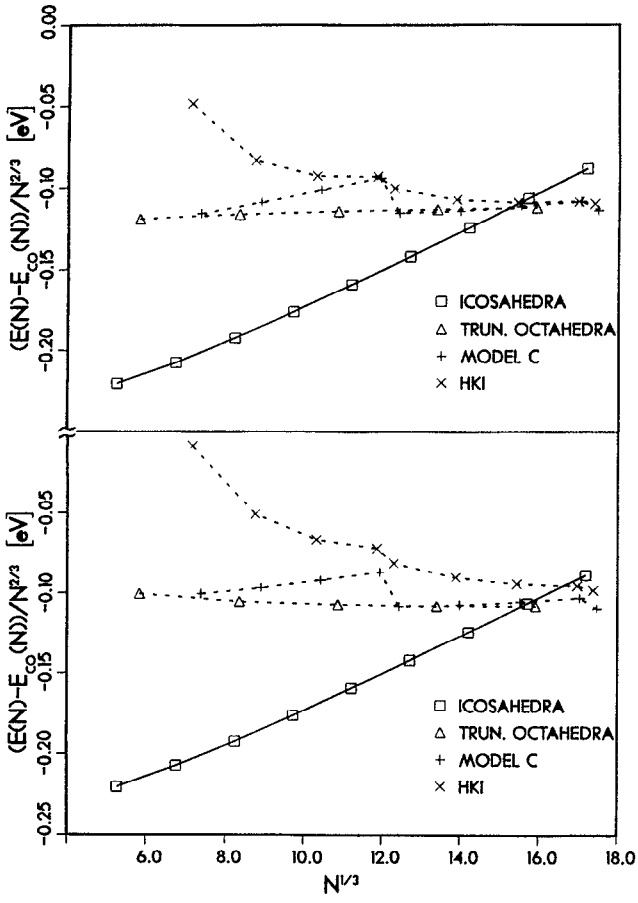

FIG. 8. In the top graph, the minimized energies of microscopic clusters are represented, relative to an interpolated cuboctahedral energy. In the bottom graph, equivalent macroscopic quantities are displayed, with the exception of the curve for icosahedra, which is the same as in the upper graph.

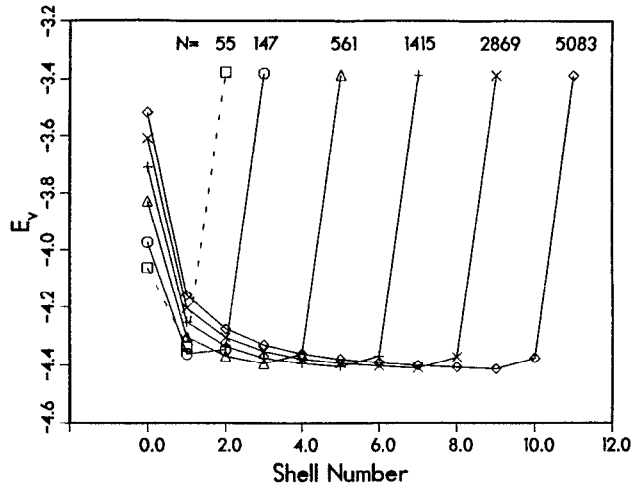

FIG. 9. The energies of vertex atoms on successive shells of icosahedra of various sizes. Lines connect energies corresponding to atoms in different shells in the same icosahedron. Results for icosahedra comprising three, five, seven, nine, and eleven shells are shown. The 55-atom, two shell icosahedron is also shown, but with a dashed line.

clusters which enables them to compete energetically as well as they do.

As mentioned above, we may analyze the energy of a cluster atom by atom. In Fig. 9 we display how the energies of atoms on the fivefold axes change as we move from the inside of a cluster to its outside. We observe a great regularity with overall cluster size if we compare the outermost layer of each cluster and then successively proceed inwards. Our overall observation is that the energies of atoms in the outer shells of these clusters are very similar, but that as the interior of the cluster is penetrated, energies increase. The further one penetrates, the greater is the increase in atomic energy with a particular concentration of energy at the center of the cluster. Since a large part of the cohesive energy in metals derives from the embedding of the metal ions in the electronic charge density of the medium, atoms will seek to occupy positions which optimize that embedding energy. Consequently, atoms on the outer shells of the cluster attempt to compensate for the missing of neighbors which would have been present in the bulk by displacing inward toward regions of higher electronic density. (The optimal structure is of course a balance between the cohesive embedding energy and the core–core repulsions.) The atoms that experience the greatest loss of electronic embedding density are the ones at the outside vertices of the cluster. Under the geometry of the icosahedron, these atoms can only move to a region of higher electronic density by pressing directly on atoms at the vertices of the shell below theirs. Because the vertex atoms form a linear chain from the outside of the cluster to its center, and since the stress on these atoms is radial, stress accumulates along the fivefold axes and especially at the clusters' centers. It is not surprising that the energy of an atom at a cluster's center is still increasing almost as strongly with the cluster's radius when the cluster has ten or 11 shells as when it had two or three. (We suspect this behavior to be largely independent of the interatomic interaction for potentials that favor close-packed structures, since the geometry of the icosahedron almost forces such a concentration of stress.)

Similar analysis to that leading to the results shown in Fig. 9 could also be made for atoms on the edges adjoining faces on shells within the icosahedra or atoms on the faces themselves. By way of definition, let us say that aside from the vertex atoms on an icosahedral shell, we also have edge atoms, which adjoin two faces, but do not include the vertex atoms, and face atoms, which include every atom that is neither a vertex or an edge atom. It is worth pointing out that although unrelaxed clusters show a considerable variation in atomic energies for the edge atoms in a shell, or for the face atoms in a shell, the edge energies are remarkably uniform within a given shell of a cluster after relaxation, as are those of the face atoms. For example, in the 11-shell, 5083 atom icosahedron, the standard deviation of energies of edge atoms is greatest for the tenth shell, where it is 0.003 27 eV, as compared with an edge average for that shell of -4.4183 eV. For the same cluster, the standard deviation of energies of face atoms is greatest for the 11th shell, where it is 0.005 02 eV, as compared to a facial average for that shell of $-3.939\,29$ eV. Within a given shell of an icosahedron, the energy difference between a pair of atoms chosen from two different categories (vertex, edge, or face) is much greater

than the energy difference between any pair of atoms within any single category.

Farges *et al.*[9] consider similar issues for clusters whose atoms interact through a Lennard-Jones 6-12 potential. They show how the spacing between pairs of adjacent atoms lying on one of the fivefold axes of an icosahedral cluster changes in moving from the inside of a cluster out, and for a given distance from the center, how it changes with cluster size. We call this spacing the radial nearest-neighbor distance. Furthermore, they examine the nearest-neighbor distance between atoms near the center of a face for each of the shells of which an icosahedral cluster is composed. We take this to mean the distance between those two atoms in the shell nearest the center of a face, whether one of the atoms is exactly in the center or not, and call it the tangential nearest-neighbor distance for that shell. In Fig. 10, we show the results for the icosahedral clusters that we have studied, which are qualitatively similar to the results of Farges *et al.* although somewhat larger in degree. We note that both the radial and tangential distances between atoms decrease nonuniformly as we move from the outside toward the inside of the cluster. Furthermore, as we consider larger and larger clusters, the distances at the surface of the clusters increase and the distances near its center decrease. For the icosahedral clusters we have examined, the radial nearest-neighbor distance is always less that the nearest-neighbor distance in a perfect bulk crystal, while the tangential nearest-neighbor distance is larger than that distance for a cluster's outer layers and smaller for its inner ones.

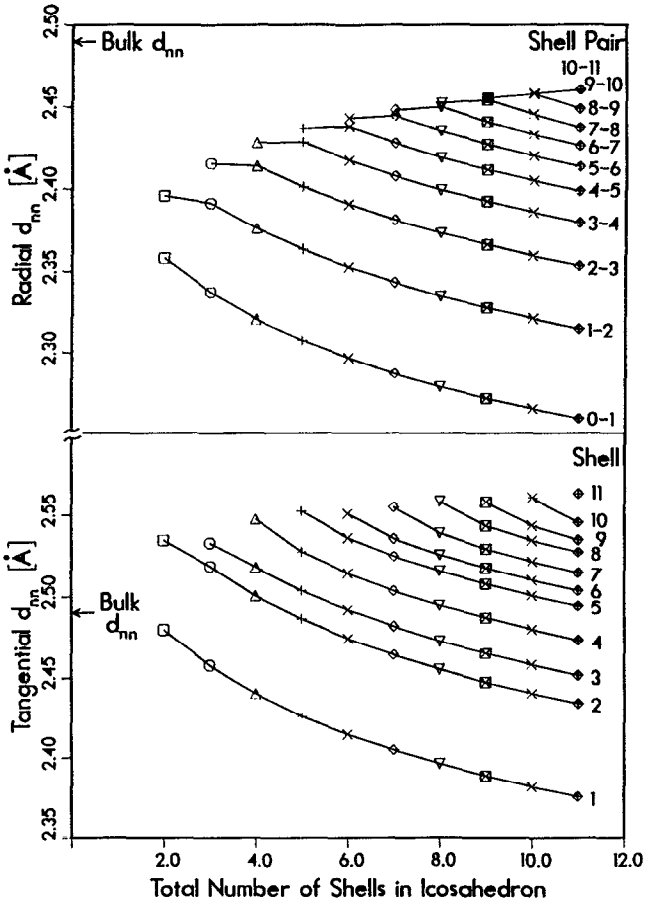

FIG. 10. In the top graph, the distances between adjacent atoms on a fivefold axis of an icoshedral cluster are shown. The curves connect distances in different clusters between atoms in the same two shells and are marked by the pair of shell numbers involved. In the bottom graph, the distance between the two atoms in a shell closest to the center of one of its faces is shown, marked by the number of the shell. Note that the numbering of shells is such that shell zero has one atom, shell one has 12, etc.

Farges *et al.*[9] also provide information about the convexity of faces on the 923-atom, six-shell icosahedral Lennard-Jones cluster and suggest that the convexity is more or less uniform from shell to shell for any given icosahedral cluster. Following their suggestion, we take a radial unit vector through the center of a face and project onto it two vectors pointing from the center of the cluster, with one pointing to a vertex atom on that face and the other pointing to the atom closest to the face's center. We define the layer position of the face to be the mean of these projected distances and the layer distortion to be their difference. We find for the six-shell icosahedral cluster that the ratio of the distortion for the outermost shell to the difference between the layer position of the two outermost shells is about 13%. Farges *et al.*, obtain 9% for an apparently similar quantity for their Lennard-Jones material. They observe that this ratio increases in a nearly linear manner with shell number if it is also calculated for the interior shells of the cluster, suggesting a uniformity of convexity throughout the shells of the cluster. We also observe a roughly linear relation between shell number and this ratio. Moreover we note that this ratio, for a given shell number within a containing icosahedral cluster, is remarkably independent of the size of the cluster containing it.

An alternative measure of the convexity of a surface may be obtained in the following manner: Let us define two spheres. One is chosen so that its center is at the center of the icosahedral cluster and its surface passes through the vertex atoms on a given shell of the cluster. The other is chosen so that its surface passes through the vertex atoms of a particular face and also through the atom closest to the center of that face (or rather through the projection of that atom's position onto the radial unit vector through the center of the face). As the mean curvature C of the face, we take the reciprocal of the radius of the second sphere, although the face will tend to be flatter in its center than at its edges. To normalize this curvature in a way that should be independent of which of the shells we are examining if they are all similar, we multiply it by the radius R_v of the first sphere. Thus if the faces were completely flat, the product would be zero, while if the cluster had relaxed to a perfect sphere, it would be unity. Results are shown in Fig. 11. We find that as expected, this relative curvature uniformly decreases as we move to larger and larger clusters, since it ultimately must conform to the macroscopic limit.

C. Decahedra

The principle difficulty in studying the energies of Marks' decahedra is the richness of the parameter space [see Figs. 4(c) and 5]. As a simplification, we ignore (110) faces

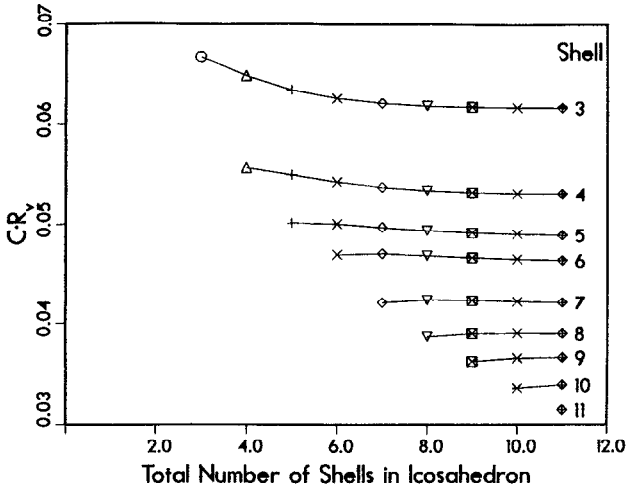

FIG. 11. The relative curvature of faces on shells within icosahedra of various sizes.

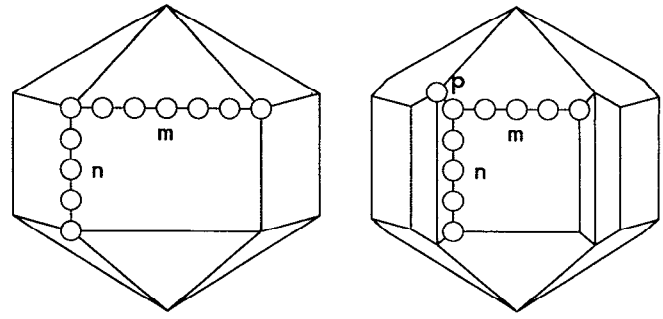

FIG. 12. An Ino's decahedron with $m = 7$ and $n = 5$ is shown on the left. On the right is shown the resulting Marks' decahedron if the outermost line of atoms on each twinning plane is removed. This decahedron has $s = 1$ and $p = 2$ as well as $m = 5$ and $n = 5$.

since in the range of cluster sizes which we study, such faces do not appear to be favorable. Even so, we have two inequivalent kinds of (111) faces, which we have called capping faces and notch faces. Thus while we can specify one of our single-crystal polyhedra without (110) faces just by listing the number of atoms on the edge joining (100) and (111) faces m and the number of atoms on the edge joining two (111) faces n, we will find an additional parameter is needed for decahedra. For decahedra, we will use m to denote the number of atoms on an edge joining a (100) face and a capping (111) face, n to denote the number of atoms on the other kind of edge on a (100) face, which connects it with either a notching (111) face or if no notching has occurred with a neighboring (100) face, and p to denote the number on an edge joining the two kinds of (111) face. This notation is the same as that used by Raoult *et al.*[8] Instead of p, however, we shall usually refer to $s = p - 1$, the number of (111) notching planes which have been removed from the sides of each decahedral unit to produce the desired Marks' decahedron. We choose to do this since our scheme for organizing the plethora of Marks' decahedra refers each back to the Ino's decahedron from which it could be made by notching, and which is simply a Marks' decahedron with $s = 0$ [see Figs. 4(b) and 4(c)]. An Ino's decahedron and any Marks' decahedron that can be obtained from it by notching all belong to the same "family." Two Ino's decahedra belong to the same family if for them $m - n$, which measures the "squareness" of the (100) face, has the same value. Thus in Fig. 12, both the Ino's decahedron and the Marks' decahedron belong to family $m - n = 2$. The Ino's decahedron has $m = 7$, $n = 5$, $s = 0$ (and $p = 1$), while the Marks' decahedron has $m = 5$, $n = 5$, $s = 1$ (and $p = 2$).

If we take any Ino's decahedron and begin notching it at the twinning planes, we find that, relative either to bulk energies or cuboctahedral energies, a sharp minimum exists. In Fig. 13 we show the results for family four, i.e., the set of decahedra arising from notching an Ino's decahedron with $m - n = 4$.

Similar calculations were performed for members of families two, six, and eight. The geometries of the decahedral clusters which we investigated are given in Table V. We observed that as one moves to larger and larger clusters, the number of the energetically optimal family increases and the degree of notching of the optimal member of that family increases as well. The results of these calculations are summarized in Fig. 14, where we display the energies for those decahedral clusters with energies lower than any other decahedron of similar size, along with the curve of microscopic icosahedral energies which we have seen in so many of the other figures. We conclude that icosahedra become unstable with respect to Marks' decahedra for clusters larger than about 2300 atoms.

In examining Fig. 14, we note that minimum energy decahedra tend to have square (100) faces and that the size of those faces and the depth of the notch embracing them increases with increasing cluster size just as we would expect from macroscopic considerations. To make the comparison with macroscopic expectations more quantitative, we show

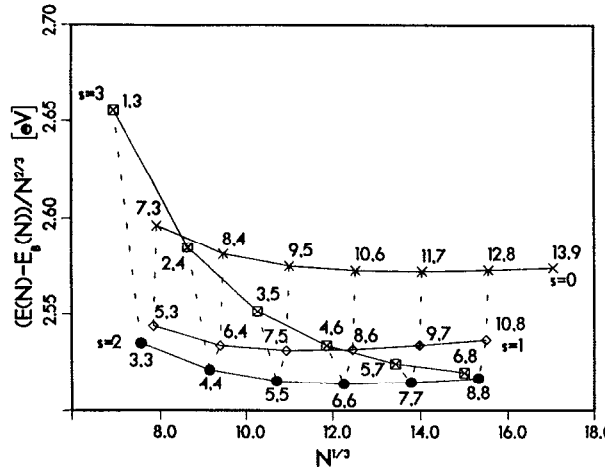

FIG. 13. The energies of the decahedral family four relative to the bulk energy of the same number of atoms. The solid lines connect members with the same degree of notching, while the dashed lines connect each cluster with that one produced from it by further notching and with its parent cluster from which it was similarly produced. The s value for each solid curve is used to denote it, while each cluster is marked by its m and n values.

TABLE V. Decahedral clusters: numbers of atoms N, number of atoms on an edge between a capping (111) and a (100) face m, number of atoms on the other type of edge on a (100) face n, and the depth of the notch s, for the decahedral families 2, 4, 6, and 8, corresponding to decahedra that may be produced by various degrees of notching from Ino's decahedra with $m - n = 2$, 4, 6, and 8, respectively.

Family 2				Family 4				Family 6				Family 8			
N	m	n	s	N	m	n	s	N	m	n	s	N	m	n	s
207	5	3	0	499	7	3	0	971	9	3	0	3397	13	5	0
409	6	4	0	851	8	4	0	1513	10	4	0	4569	14	6	0
711	7	5	0	1333	9	5	0	2215	11	5	0	5971	15	7	0
1133	8	6	0	1965	10	6	0	3097	12	6	0				
1695	9	7	0	2767	11	7	0	4179	13	7	0				
2417	10	8	0	3759	12	8	0	5481	14	8	0				
3319	11	9	0	4961	13	9	0	1493	8	4	1				
4421	12	10	0	484	5	3	1	2190	9	5	1				
192	3	3	1	831	6	4	1	3067	10	6	1				
389	4	4	1	1308	7	5	1	4144	11	7	1				
686	5	5	1	1935	8	6	1	1428	6	4	2				
1103	6	6	1	2732	9	7	1	2110	7	5	2				
1660	7	7	1	3719	10	8	1	2972	8	6	2				
2377	8	8	1	434	3	3	2	4034	9	7	2				
3274	9	9	1	766	4	4	2	1308	4	4	3				
4371	10	10	1	1228	5	5	2	1965	5	5	3				
142	1	3	2	1840	6	6	2	2802	6	6	3				
324	2	4	2	2622	7	7	2	3839	7	7	3				
606	3	5	2	3594	8	8	2	1745	3	5	4				
1008	4	6	2	339	1	3	3	2547	4	6	4				
1550	5	7	2	646	2	4	3	3549	5	7	4				
2252	6	8	2	1083	3	5	3								
3134	7	9	2	1670	4	6	3								
4216	8	10	2	2427	5	7	3								
461	1	5	3	3374	6	8	3								
838	2	6	3												
1355	3	7	3												
2032	4	8	3												
2889	5	9	3												
3946	6	10	3												

results for family four in Fig. 15, where in the macroscopic calculations the surface planes are taken to cut through surface atoms. In the upper panel energies obtained via microscopic, atomistic energy minimizations are shown relative to

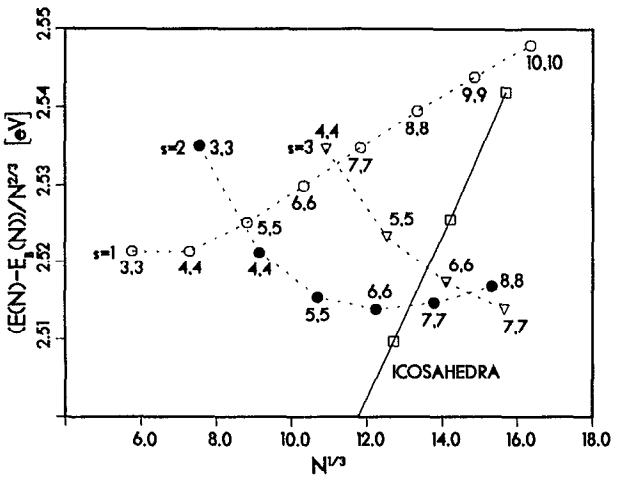

FIG. 14. Those decahedral sequences we have studied which have somewhere an energy lower than any other decahedral sequence of corresponding size. Each curve is marked with its degree of notching s and each decahedron's point is marked with its m and n values. The icosahedral curve, obtained from microscopic energy minimization, is included for comparison.

cuboctahedral energies, and in the lower panel, the corresponding macroscopic results are displayed. For reference, the microscopic icosahedral energies are shown in the upper graph. We find excellent agreement between the ordering provided by the macroscopic calculations and the microscopic results. In evaluating the quality of the decahedral results, it should be borne in mind that the decahedra used in the macroscopic calculation are made from unrelaxed, classic decahedra and not macroscopic decahedra whose geometries are consistent with the bulk system whose energy we minimized under decahedral strain. Using the latter geometries instead results in an overall lowering of the macroscopic energies, reducing the overall energy shift between the two panels of Fig. 15.

D. Other clusters

In addition to the above structures, other model structures of atomic clusters have been examined in order to check that we have indeed considered most of the structural motifs relevant to our study of the energetics of nickel clusters. Thus, e.g., we have studied "model B" of Raoult *et al.*,[8] which is a shift from the truncated octahedron in the opposite direction to that taken by model C, so that it has smaller (100) faces. As expected, this is energetically quite unfavorable. Furthermore, unlike the Lennard-Jonesium clusters of Raoult *et al.*,[8] removing the 12 vertex atoms on the icosahe-

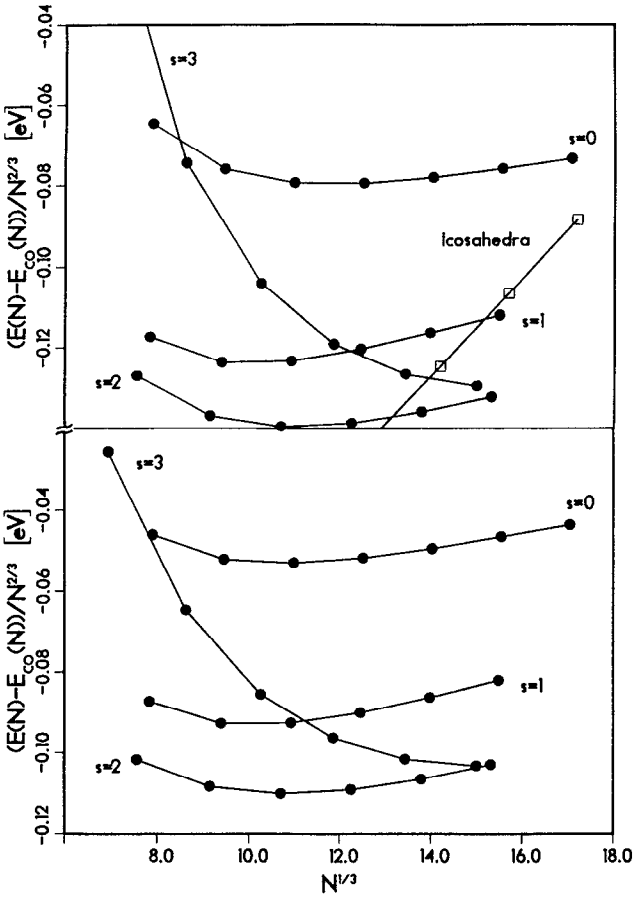

FIG. 15. In the upper graph the minimized microscopic energies for family four are represented relative to the cuboctahedral energy. In the lower figure, the corresponding macroscopic results are shown, where we have taken each surface's plane to pass through its atoms. The microscopic results for the icosahedron (squares) are shown in the upper graph as well.

dral clusters makes them worse competitors energetically. This type of variation never seems to be advantageous for any cluster types and we have not systematically explored it. We have also created monotwins of some of the single crystals, which invariably lowered the cluster's energy, but to a degree so small compared to other energy differences as to be uninteresting. For example, the untwinned HKI cluster with 3679 atoms has a total energy of $-15\,766.341$ eV. The corresponding twinned cluster has a total energy only 0.086 eV, or 0.28 K lower.

There is another large group of clusters that we have not extensively studied simply because they are too numerous: those with broken symmetry, i.e., clusters with incomplete shells, or those hybridized from pieces of several clusters of the more symmetric type which we have considered. Such clusters may be abundant under experimental conditions. For example, for clusters produced via a laser-vaporization cluster source, where at low helium pressures the principal mechanism of cluster growth is by monomer addition, the odds that the number of atoms in a cluster turns out to be one of the values for which an energetically optimum, symmetric shape can be made are small. Similarly, for clusters which evolve from molten droplets, evaporation of excess atoms will essentially cease prior to any solidification because of the large binding energy for surface atoms (~ 3.5 eV).

The systematic trends revealed from our study of the more symmetric structural forms guide us as to which structures may develop when the number of atoms in a cluster does not correspond to one of the symmetric structures which we have considered. The easiest way to interpolate numbers of atoms is by breaking the symmetry of the clusters. One could use model C type faces on part of a cluster's surface and those from a truncated octahedron elsewhere. If somewhat fewer atoms are required, some vertex atoms might be removed, or if the cluster is big enough, some (110) faces applied. In the decahedra, there may be variation among the five tetrahedral units. In general, the surface of each single crystal piece will attempt to resemble a piece from the Wulff polyhedron even for clusters that are quite small. Exceptions are the icosahedra, where we expect that the best clusters of lower symmetry will have an icosahedral core with a partial outer shell whose atoms are as compactly arranged as possible. To avoid energetically expensive sharp atomic steps on a cluster's surface, the simplest procedure is to take a larger cluster in the family in question and remove whole atomic planes at a time. It is worth pointing out that the truncated octahedra, model C's, and HKI are all single-crystal clusters related to each other by just such operative transformations and, except for the HKI clusters of small sizes, all have similar energies. This indicates that interpolation between similar high-symmetry configurations may provide some information about energies of clusters of intermediate sizes.

In order to illustrate these ideas, we have considered clusters with 201 atoms. Of the high-symmetry structures which we have studied so far, only a truncated octahedron can have exactly this many atoms. On the other hand, as we see from the upper half of Fig. 7, the icosahedra have a much lower scaled energy than the truncated octahedra in this size range ($N^{1/3} \sim 6$). The question naturally arises as to whether some less symmetric icosahedrally based cluster with 201 atoms might be lower in energy than the highly symmetric truncated octahedron.

A cluster with the desired number of atoms may be constructed by adding extra atoms to a 147-atom icosahedron or removing excess atoms from a 309-atom icosahedron. For the purpose of our illustration, we have chosen the second construction, attempting to remove whole planes of atoms at a time. Accordingly, starting from a 309-atom icosahedron, we pick a vertex and remove all five surface planes that meet at it, exposing part of the 147-atom core. We continue this process by removing planes of atoms on facets adjacent to the area we have already cleared until we have 201 or less atoms left. In fact, following this procedure results in our case in a cluster containing 200 atoms to which one atom is replaced at the edge of the partial shell which caps the 147-atom icosahedral core. Direct minimization of the energy of that cluster yields a total energy $E(N) = -807.076$ eV which is slightly below that of the corresponding 201-atom truncated octahedron (-807.003 eV). The resulting cluster is shown, front and back, in Fig. 16, where atoms belonging to the 147-atom icosahedral core are light gray and those

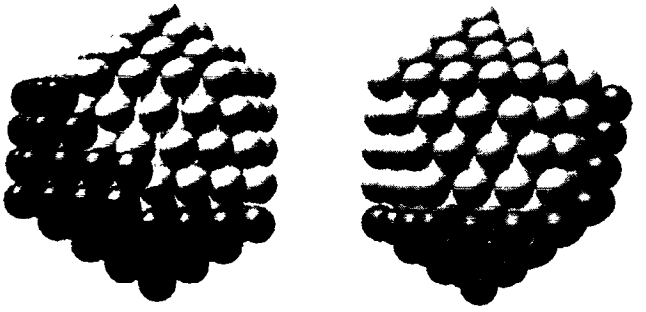

FIG. 16. Front and back views of a low symmetry 201-atom cluster with an icosahedral core of 147 atoms (light gray) and a capping partial shell of 54 atoms (dark gray) constructed as detailed in the text.

of the capping partial shell are dark gray (the extra 201st atom is the dark gray one nearest the center of the left image). It is of interest to note that the effect of this extra atom is rather large. The energy of the corresponding 200-atom icosahedrally based cluster is -803.353 eV, while that of the 201-atom truncated octahedron with one of its vertex atoms removed is -802.589 eV, markedly increasing the energetic advantage of the icosahedrally based cluster as compared with the 201-atom case.

We would like to note that other construction methods that we have attempted, including some which involved molecular dynamics simulated annealing, resulted in clusters of substantially higher energy than the one which we have demonstrated here. While we have undoubtedly not exhausted all the possible construction schemes, our result indicates that it is possible to achieve energetically competitive low-symmetry clusters by starting from judiciously chosen high-symmetry structures and removing whole atomic planes at a time, as discussed above. Our general conclusion is that in attempting to build low-symmetry clusters whose number of atoms is incompatible with high-symmetry structures, the energy differences between the latter (such as displayed in Fig. 8) provide guidance in choosing the high-symmetry structural motif on which to base the construction of the low-symmetry clusters.

V. SUMMARY

In this paper we have investigated using both a macroscopic approach and atomistic energy minimizations, the size dependence of the evolution of structures in metal (nickel) crystallites ranging in size from small clusters containing tens of atoms to rather large ones made of thousands of atoms. In our studies we have used many-body interaction potentials obtained via the embedded atom method (see Sec. II), which include as a dominant contribution to the cohesive energy of the metal the embedding energy of the metal ions in the local electron density provided by the other atoms in the system. In addition, we compare our results to those obtained previously, employing simple pair-potential models.

One of the aims of our study is to test and assess the adequacy of macroscopic concepts based on the Wulff construction and variants thereof [i.e., considerations of elastic energies and the modified Wulff construction due to Marks[19] (see Sec. III)]. Based on comparisons between the results of atomistic energy minimization and the macroscopic formulas which we developed [see Eqs. (4), (5), and (B1)], we conclude that these formulas, in conjunction with accurately calculated, or experimentally measured, cohesive, surface, and strain energies [which in our studies were obtained using the EAM potentials (see Secs. II and III, and the Appendices] allow a rather reliable framework for structural analysis. The macroscopic approach is particularly useful in assessing the relative energetic merits of various structural motifs (see the comparisons between the results of microscopic and macroscopic calculations in Sec. IV) and thus aids in the analysis of experimental data.

The evolution with size of the optimal structures of nickel, as well as Lennard-Jonesium (after the results of Ref. 8) clusters is summarized in Fig. 17. As seen from Fig. 17(a), our microscopic, atomistic calculations based on the EAM many-body interactions predict that the optimal structures of nickel clusters containing less than ~ 2300 atoms belong to the icosahedral sequence. Larger clusters are predicted to optimally assume Marks' decahedral geometries, while for clusters containing more than $\sim 17\,000$ atoms, single crystal structures and their monotwins are energetically favored. Observe that we predict, on a macroscopic basis, that the evolution of optimal structures from the decahedral sequence to the single crystal sequence happens for much smaller cluster sizes for nickel that has been predicted[8] for Lennard-Jonesium, where on the order of 10^5 atoms are expected to be necessary. The transition for ener-

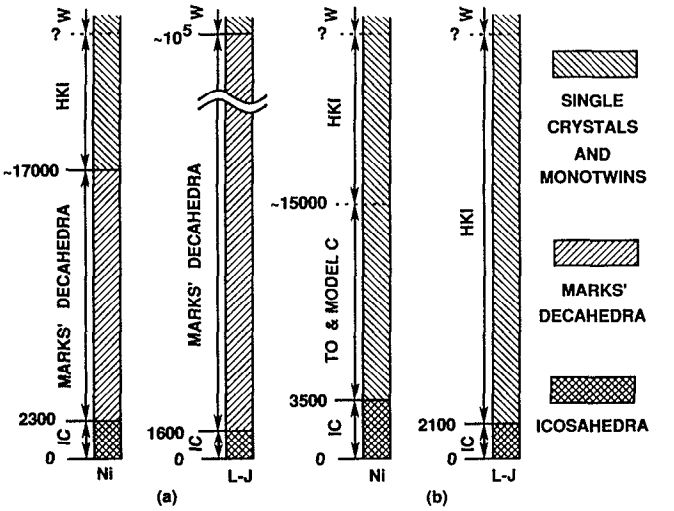

FIG. 17. Diagrams, summarizing the evolution of optimal structural motifs, vs the number of atoms in nickel clusters (obtained in this study) and in Lennard-Jonesium (after the results of Ref. 8). The results in (a) correspond to calculations including in the set of possible structures those of Marks' decahedra. The results in (b) were obtained without the inclusion of Marks' decahedra in the set of possible structures. Solid lines divide structures which belong to different internal structural forms (icosahedra, denoted by IC; Mark's decahedra; and the single crystals and their monotwins, denoted by TO for truncated octahedra, model C, HKI, or W for other Wulff-type structures). Dashed lines divide structures which have the same internal form, but differ in their surface configuration (these are all single crystals and their monotwins).

getically favored structures between the icosahedral sequence and the Marks' decahedral sequence is predicted to occur for somewhat larger clusters in nickel than for Lennard-Jonesium (2300 vs 1600 atoms[90]). In this context, we remind the reader that the HKI, model C, and truncated octahedron are all single crystal clusters (see Sec. IV A) and they all serve as approximations, forced by the discrete nature of matter, of the Wulff shape. As clusters become larger and larger, it becomes less and less useful to distinguish between clusters that only differ between one another by the addition or removal of a single plane or row of atoms, and we may just as well speak of the Wulff sequence, or that set of cluster structures that are good approximations to the Wulff polyhedron. On the other hand, Marks' decahedra, which are based on fivefold symmetrical structures, do not belong either to the single crystal structures, or the icosahedral structures.

The diagrams for nickel and Lennard-Jonesium in Fig. 17(b) summarize the structural evolution vs size when Marks' decahedra are not considered. As seen, such calculations predict the emergence of single crystal structural motifs (i.e., truncated octahedra, model C, and HKI) as optimal clusters for much smaller sizes than when Marks' decahedra are included, while the cluster size for the icosahedral to single crystal transition in nickel (3600 atoms) is substantially greater than that for Lennard-Jonesium (2100 atoms[91]).

For the case of icosahedral structures, we find that the effect of relaxation (obtained by atomistic minimization) of these clusters from the "ideal" structure given by the macroscopic approach is much larger than is the case for decahedral and single crystal structures. These relaxations of icosahedral clusters lead to relief of strain by nonuniform relaxations of atoms in the cluster, resulting in curved (i.e., nonflat) facets. Furthermore, the convexity of the structure propagates into the interior of the cluster (see Sec. IV B).

While in this study we focus on structural motifs of high symmetry, we also demonstrate that the results which we obtained can guide the construction of energetically competitive low-symmetry clusters.

In closing, we reiterate that the results presented in this paper do not include thermal (and entropic) effects, which can lead to isomerizations between accessible structural forms and thus to a distribution of structures for a given size cluster. While a more comprehensive account of the behavior of nickel clusters at finite temperatures will be given elsewhere, it is instructive, within the context of this study, to comment on the stability of these clusters at finite temperatures. As seen by molecular dynamics simulations which we have performed, almost all the types of clusters which we have considered here are stable up to the temperature at which their surface atoms begin to diffuse and the clusters can start to isomerize, generally ~ 1000 K depending on cluster size.

The exceptions are clusters which can convert to another of lower energy via a cooperative, nondiffusive transformation, i.e., the one which connects cuboctahedra and icosahedra. We have observed that on heating, cuboctahedra undergo the multitwinning transformation well before any atomic diffusion occurs, resulting in icosahedra.

As the temperature is successively increased further, more outer layers melt and wet a structurally unchanged solid core (i.e., states of coexistence between liquid, or quasiliquid, and solid phases occur). Finally, if enough energy is added, the cluster will melt completely.

ACKNOWLEDGMENTS

This research is supported by the U.S. Department of Energy (DOE) under Grant No. FG05-86ER-45234. Portions of the computations were carried out at the Florida State University Computing Center through a DOE grant of computer time.

APPENDIX A: UNIFORM DECAHEDRAL STRAIN

In this appendix, we will show how the surface, twinning, and strain energies needed for a macroscopic calculation of the energy of one of Marks' decahedra were obtained. In Fig. 18, we display an unstrained unit cell with the tetrahedral unit embedded in it. The periodic repetition of this cell under the three translation vectors **a**, **b**, and **c** will fill all space. Each of these three vectors points in a (100) direction. In order to change this unit cell into one containing a tetrahedral unit that will fit into a decahedron, we must change these three vectors, so that they satisfy certain constraints.

We will choose to proceed so that the (100) surface created by removing the periodic boundary condition in the **c** direction corresponds to the (100) surfaces that occur on Ino's or Marks' decahedra. Then the line AB on the tetrahedron will correspond to the decahedral axis. Our first constraints come from the requirement that the lengths of AC, BC, AD, and BD must all be the same. In terms of the transla-

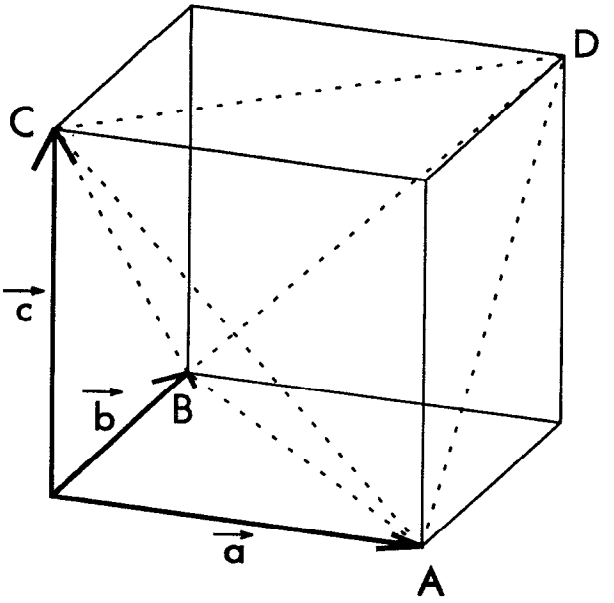

FIG. 18. An unstrained computational cell for fcc crystals. The three vectors **a**, **b**, and **c** are translations under whose repeated application the computational cell periodically fills all space. They are currently pointing in (100) directions. We will apply decahedral strain by changing these three vectors to ones consistent with decahedral symmetry.

tion vectors, this implies that

$$a = b \tag{A1}$$

and

$$\mathbf{c}\cdot\mathbf{a} = \mathbf{c}\cdot\mathbf{b} = 0. \tag{A2}$$

We conclude that without loss of generality we can choose **c** to lie in the $+z$ direction and **a** and **b** to line in the x–y plane. Further, since we can rotate the resulting setup about the z axis without changing the system's energy, we can further take one of either a_y or b_x zero. If, as is usual, we write the three translation vectors as column vectors and take them as the columns of an overall translation matrix **H**,

$$\mathbf{H} = (\mathbf{a},\mathbf{b},\mathbf{c}), \tag{A3}$$

we could so far choose to write **H** as

$$\mathbf{H} = \begin{pmatrix} a_x & \sqrt{(0,a_x^2 - b_y^2)_+} & 0 \\ \sqrt{(0,b_y^2 - a_x^2)_+} & b_y & 0 \\ 0 & 0 & c_z \end{pmatrix}, \tag{A4}$$

where $(\alpha,\beta,\gamma,\ldots)_+$ is the supremum of α, β, γ,.... This expression could be simplified by simply asserting that **a** lies along the x axis so that $a_y = 0$, corresponding to the case where $a_x \geqslant b_y$, but the conjugate gradient procedure will treat a_x and b_y as the two independent quantities in **H**, and we cannot be sure that it may not try to make b_y larger than a_x during minimization and must allow for that possibility.

The last constraint is of course the requirement that the dihedral angle between the ABC and the ABD planes be 72°. In terms of the translation vectors, this requirement may be written as

$$\frac{[\mathbf{c} - (\mathbf{a}+\mathbf{b})/2]\cdot[\mathbf{c} + (\mathbf{a}+\mathbf{b})/2]}{|[\mathbf{c} - (\mathbf{a}+\mathbf{b})/2]||[\mathbf{c} + (\mathbf{a}+\mathbf{b})/2]|} = \cos(72°). \tag{A5}$$

Equations (A4) and (A5) allow us to determine c_z in terms of a_x and b_y. We find

$$c_z = \nu\sqrt{\left[a_x + \sqrt{(0,a_x^2 - b_y^2)_+}\right]^2 + \left[b_y + \sqrt{(0,b_y^2 - a_x^2)_+}\right]^2}, \tag{A6}$$

where

$$\nu = 0.5\sqrt{[1 + \cos(72°)]/[1 - \cos(72°)]} = 0.6882\ldots . \tag{A7}$$

That we have only two degrees of freedom left is exactly as expected. We can volumetrically expand or contract a decahedron or change the length of its axis and we will still have a decahedron. Other kinds of changes to the tetrahedral units will either prevent them from joining together or create mismatches between their edges and vertices.

We can now fill this computational cell with an "fcc" lattice of 500 nickel atoms arranged so that there are five conventional unit cells in the **a** direction, five in the **b** direction, and five in the **c** direction, and then minimize the energy by allowing a_x and b_y to vary with the other components of **H** then being determined as in Eqs. (A4) and (A6). Comparing the resulting energy with the bulk energy of the same number of atoms in a perfect, unstrained fcc crystal gives us the strain energy.

The Parrinello–Rahman method[77] returns the derivative of the potential energy with respect to each of the nine components of **H** disregarding any constraints on them. It is a small detail that we must use the chain rule to determine from these derivatives the derivatives with respect to a_x and b_y with constraints in place. For a_x we have

$$\frac{\partial V}{\partial a_x} = \sum_{i=1}^{3}\sum_{j=1}^{3} \frac{\partial V}{\partial H_{ij}}\frac{\partial H_{ij}}{\partial a_x}. \tag{A8}$$

Parrinello–Rahman methods give us the first partial derivative in the sum and Eqs. (A4) and (A6) give us the second. b_y is of course treated in the same way.

We may remove the periodic boundary condition in the **c** direction and minimize the energy of the resulting slab by varying atomic positions within a fixed computational cell, obtaining the (100) surface energy under decahedral strain.

Unfortunately, the system as described is not well suited to determining the (111) surface energies or twinning energies, since it is not easy to create the appropriate interfaces. It might appear that we need to go to a different kind of computational cell for which (111) surfaces can be easily made, such as the one in Fig. 3, reexamine the consequences of the constraints needed for decahedral symmetry, and reminimize the bulk energy under those constraints, but we do not.

Any translationally periodic system may have its periodicity represented through any three noncollinear periodic translation vectors. Imagine that the computational cell in Fig. 18 corresponds to the one that was produced by the minimization procedure—the changes are very small and do not justify a second figure. Instead of describing the periodicity of this bulk system by using **a**, **b**, and **c**, we could just as well have used

$$\begin{aligned} \mathbf{a}' &= \mathbf{c} - \mathbf{a}, \\ \mathbf{b}' &= \mathbf{c} + \mathbf{b}, \\ \mathbf{c}' &= \mathbf{b} - \mathbf{a}. \end{aligned} \tag{A9}$$

In terms of Fig. 18, $\mathbf{a}'$ points from A to C, $\mathbf{b}'$ points from A to D, and $\mathbf{c}'$ points from A to B. This is a right-hand coordinate system analogous to the one in Fig. 3 and is suited for a calculation of the (111) surface energy. Just as there the three vectors define a tetrahedron, here they define $ABCD$. The new parallelepiped unit cell has a volume that is twice that of the old one, so it is unsurprising that when we periodically replicate the atomic positions in the old one to see which copies fall in the new one we find that 1000 copies do. At this point on it is probably better to refer to Fig. 3, where **a**, **b**, and **c** can play the role of $\mathbf{a}'$, $\mathbf{b}'$, and $\mathbf{c}'$.

These 1000 atoms are arranged as ten (111) layers parallel to the sides of the computational cell, whether we scan through the system along the $\mathbf{a}'$, the $\mathbf{b}'$, or the $\mathbf{c}'$ direction. Unfortunately, the stacking sequence for (111) layers in an fcc crystal only repeats every third layer, which means the new system will contain serious stacking faults if periodically repeated. Fortunately this is easily repaired. We simply reduce the three new translation vectors by 10% and only keep the copies of atoms which fall in this newer, smaller cell. We find that 9^3 do. Replicating these 729 remaining atoms in this newest unit cell with its periodic translation vectors produces exactly the same atomic coordinates as replicating the original 500 atoms with the original, relaxed translation vectors: they are equivalent periodic systems. Thus we have constructed a system with decahedral strain with periodic translation vectors suitable for determining energies involving (111) planes.

In terms of Fig. 3, the two planes *OAC* and *OBC* meet at the line *OC* with a dihedral angle of 72°. Thus these two planes have the proper orientation for either a twinning plane or a notching (111) face. The other two faces of the tetrahedron *OAB* and *ABC* have the orientation of capping (111) faces. Thus by removing the periodic boundary condition in the $\mathbf{c}'$ direction, we can determine the surface energy of the capping (111) faces by minimizing the energy of the resulting slab while holding the computational cell fixed and comparing the resulting energy with that of the bulk slab *under decahedral strain*. Similarly, by removing the periodic boundary condition in the $\mathbf{b}'$ direction, we can determine the surface energy of the notching (111) face. Leaving both periodic boundary conditions in place, we can introduce two twinning planes in the original bulk system. Look at the system as a set of nine atomic (111) planes parallel to the $\mathbf{a}'$–$\mathbf{c}'$ plane. These have a stacking sequence *abcabcabc*, counting away from the $\mathbf{a}'$–$\mathbf{c}'$ plane. Let us take the last four of these and rotate them 180° about their normals and put them back so that stacking sequence is *abcabCbaCabc*..., where we have periodically extended the sequence and indicated the twinning planes with capital letters for clarity. These two twinning planes are quite close together, but the twinning energy will turn out to be so small that there is little point in being more careful. We can now reminimize the bulk energy in the presence of these twinning planes, and by comparing the resulting minimum energy with the energy of the bulk system under decahedral strain we can determine the twinning energy appropriate to the decahedron.

The numerical results for nickel, obtained by the above method, may be found in Table III.

APPENDIX B: ENERGY OF IDEAL DECAHEDRA

In this section, we will walk through a calculation using the modified Wulff construction of the energy of a Marks' decahedron given the energy results of the previous appendix. However, instead of carrying out the construction for an unstrained single crystal, it is appropriate to carry it out for a crystal under uniform decahedral strain. Thus the normals to the surfaces will not quite point in the same directions as they would were no strain applied, and the faces will be of different sizes. Because the bulk strain energy is so small, this can make a very large difference in our estimate of the size these clusters must be before single crystal clusters or monotwins of the same size are energetically preferable.

We will neglect (110) faceting, for reasons discussed in the section on macroscopic calculations. All distances in this section will be in units of u_N, introduced in that same section.

From the computational cell which gave the lowest bulk energy for the given constraints, we know the normals to the (100) plane, as well as the (111) capping plane and the (111) twinning and notching planes. From the surface energies we found, we know how far each surface plane should be from the origin. Thus if $\mathbf{n}$ is the unit vector normal to a surface whose surface energy is γ, a point $\mathbf{r}$ can be on the plane if it satisfies $\mathbf{n}\cdot\mathbf{r} = \gamma$. If we have another plane adjoined to this one at an edge, the equations of the edge follow from the requirement that the equations of both planes must be simultaneously satisfied, and a vertex where two edges meet is at a point where the two sets of equations describing the edges hold simultaneously. Thus the determination of all the coordinates of all the vertices is a straightforward exercise. In the case of the decahedron, we only have three different vertices to find: a vertex of the (100) face; the vertex where the capping faces meet; and where a twinning plane, notching face, and capping face all meet.

Let us take a coordinate system with the origin at the center of the polyhedron and where the z axis runs along what will be the axis of the decahedron (we simply take the twinning energy to be zero for the purposes of performing the modified Wulff construction). We take the x axis to be in the (100) direction and thus passing through the center of a (100) face. We place the y axis so that a right-handed orthogonal coordinate system is created.

Looking at the (100) face whose outward normal is in the $+x$ direction, we find that one of its vertices is at (0.1029, 0.0417, 0.0421), the other four being given by changing the sign on one or both of the y and z components. Notice that the height of the (100) face exceeds its width. This is not much affected by the very small energy differences between the capping and notching (111) faces, but arises because the notching planes are more parallel to the (100) plane under decahedral strain than the capping planes are and therefore cut more deeply into it. It is interesting that stretching the crystal out laterally to make it fit the decahedron makes its (100) face narrower rather than wider.

The vertex where the (upper) capping faces meet is found at (0, 0, 0.1165). The lower capping faces meet at a point just like the upper one with the sign on the z coordinate changed.

A vertex at the top of the notch, where capping, twinning, and notching (111) planes all intersect, is at (0.0801, 0.5821, 0.0586). Others of its kind may be generated by reversing one or both of the signs on the y and z coordinates. And of course, for each vertex on the decahedron, there is another that can be found by rotating the decahedron about the z axis by a 72° angle.

With explicit coordinates for all the vertices, we can certainly calculate the areas of each type of face with a little plane geometry, as well as the volume of the decahedron. On

the way we discover that the width and height of the (100) face are 0.0833 and 0.0842, respectively, while the height of the notch at its center is 0.1172 and the width of one of the notch's faces is 0.0282. The width of the capping face at its widest point is 0.1164, slightly smaller that the height of the notch as we should expect by now, and the length of the decahedron's axis is 0.2330. While the notching plane normal makes an angle with the (100) plane normal of 54° as it must, the capping plane normal makes an angle of 54.13° with it. For reference, in the unstrained crystal, both of these angles would be 54.74°, and in an unrelaxed classic decahedron, the capping plane's angle with the (100) direction would be 52.62°.

Equating the known bulk density under strain and equating it to N, the number of particles that may be in the decahedron, divided by the decahedron's volume in units of u_N cubed, allows us once more to find a connection between u_N and N, specifically $u_N = 13.1607N^{1/3}$ Å.

The area in units of u_N^2 of a single notch face is 0.002 837, so in all, the notch surface area is 0.028 37. The area of a single capping face is 0.008 564, so all the capping faces have a combined area of 0.085 64. The area of a (100) face is 0.007 018 for a combined total (100) area of 0.035 09 and the area of a twinning plane is 0.017 34 for a total twinning plane surface area of 0.1734.[92]

Combining the bulk energy for N particles, including strain energy, together with the surface areas and energies of the ten capping faces, ten notching faces, ten twinning planes, and five (100) faces, we finally find the energy of a decahedron of N particles in electron volts.

$$E_D(N) = (\epsilon_B + \epsilon_\sigma^D)N + 2.493\,87N^{2/3}, \qquad \text{(B1)}$$

where the uniform strain energy per atom of the decahedron $\epsilon_\sigma^D = 1.124\,426 \times 10^{-3}$ eV.

[1] *Elemental and Molecular Clusters*, edited by G. Benedek and M. Pacchioni (Springer, Berlin, 1988).
[2] *Physics and Chemistry of Small Clusters*, edited by P. Jena, B. K. Rao, and S. N. Khanna (Plenum, New York, 1987).
[3] *Atomic and Molecular Clusters*, edited by E. R. Bernstein (Elsevier, Amsterdam, 1990).
[4] *Mircoclusters*, edited by S. Sugano, Y. Nishina, and S. Ohnishi (Springer, Berlin, 1987).
[5] B. Raoult and J. Farges, Rev. Sci. Instrum. **44**, 430 (1973).
[6] J. Farges, B. Raoult, and G. Torchet, J. Chem. Phys. **59**, 3454 (1973).
[7] J. Farges, M. F. de Feraudy, B. Raoult, and G. Torchet, J. Chem. Phys. **78**, 5067 (1983).
[8] B. Raoult, J. Farges, M. F. de Feraudy, and G. Torchet, Philos. Mag. B **60**, 881 (1989); see also references therein.
[9] J. Farges, M. F. de Feraudy, B. Raoult, and G. Torchet, Adv. Chem. Phys. **70**, 45 (1988).
[10] L. S. Bartell, Chem. Rev. **86**, 491 (1986).
[11] S. Ino, J. Phys. Soc. Jpn. **21**, 346 (1966).
[12] K. Kimoto and I. Nishida, J. Phys. Soc. Jpn. **22**, 940 (1967).
[13] R. Uyeda, J. Cryst. Growth **24/25**, 69 (1974).
[14] E. Gillet and M. Gillet, Thin Solid Films **15**, 249 (1973).
[15] J. G. Allpress and J. V. Sanders, Surf. Sci. **7**, 1 (1967).
[16] M. Gillet, J. Cryst. Growth **36**, 239 (1976).
[17] C. Solliard, P. Buffet, and F. Faes, J. Cryst. Growth **32**, 123 (1976).
[18] L. D. Marks and D. J. Smith, J. Cryst. Growth **54**, 425 (1981).
[19] L. D. Marks, J. Cryst. Growth **61**, 556 (1983).
[20] L. D. Marks, Surf. Sci. **150**, 358 (1985).
[21] A. Howie and L. D. Marks, Philos. Mag. **49**, 95 (1984).
[22] L. D. Marks, Philos. Mag. A **49**, 81 (1984).
[23] S. Iijima in Ref. 4; see also references therein.
[24] M. J. Yacaman, K. Heinemann, C. Y. Yank, and H. Poppa, J. Cryst. Growth **47**, 187 (1979).
[25] J.-O. Bovin, R. Wallenberg, and D. J. Smith, Nature **317**, 47 (1985).
[26] A. K. Petford-Long, N. J. Long, D. J. Smith, L. R. Wallenberg, and J.-O. Bovin in Ref. 2.
[27] K. Sattler in Ref. 2.
[28] G. Apai, J. F. Hamilton, J. Stohr, and A. Thomson, Phys. Rev. Lett. **43**, 165 (1979).
[29] H. J. Wasserman and J. S. Vermaak, Surf. Sci. **32**, 168 (1972).
[30] W. Vogel, Surf. Sci. **156**, 420 (1985).
[31] A. Balerna, E. Bernieri, P. Picozzi, A. Reale, S. Santucci, E. Burattini, and S. Mobilio, Surf. Sci. **156**, 206 (1985).
[32] S. D. Berry, S. B. Dicenzo, and E. H. Hartford, Jr., Phys. Rev. B **38**, 8465 (1988).
[33] M. R. Hoare, Adv. Chem. Phys. **40**, 49 (1979).
[34] M. R. Hoare and P. Pal, Adv. Chem. Phys. **20**, 161 (1971).
[35] M. R. Hoare and P. Pal, Adv. Chem. Phys. **24**, 645 (1975).
[36] M. R. Hoare and J. McInnes, Faraday Discuss. Chem. Soc. **61**, 12 (1976).
[37] M. R. Hoare and J. McInnes, Adv. Phys. **32**, 791 (1983).
[38] C. L. Briant and J. J. Burton, J. Chem. Phys. **63**, 2045 (1975).
[39] J. Kaelberer and R. D. Etters, J. Chem. Phys. **66**, 3233 (1977).
[40] B. W. van de Waal, J. Chem. Phys. **90**, 3407 (1989).
[41] G. L. Griffin and R. P. Andres, J. Chem. Phys. **71**, 2522 (1979).
[42] H.-G. Fritsche, Phys. Status Solidi **143**, K11 (1987).
[43] J. D. Honeycutt and H. C. Andersen, J. Chem. Phys. **91**, 4950 (1987).
[44] J. W. Lee and G. D. Stein, J. Phys. Chem. **91**, 2450 (1987).
[45] S.-W. Wang, L. M. Falicov, and A. W. Searcy, Surf. Sci. **143**, 609 (1984).
[46] J. Farges, J. Cryst. Growth **31**, 79 (1975).
[47] T. Hayashi, T. Ohno, Y. Shigeki, and R. Uyeda, Jpn. J. Appl. Phys. **16**, 705 (1977).
[48] J. Farges, M. F. de Feraudy, B. Raoult, and G. Torchet, Surf. Sci. **106**, 95 (1983).
[49] J. Koutecky and P. Fantucci, Z. Phys. D **3**, 147 (1986) (a recent review).
[50] T. H. Upton, J. Chem. Phys. **86**, 7054 (1987).
[51] M. Drechsler and J. Nicholas, J. Phys. Chem. Solids **28**, 2609 (1967).
[52] M. B. Gordon, F. Cyrot-Lackmann, and M. C. Desjonqueres, Surf. Sci. **80**, 159 (1979).
[53] S. N. Khanna, J. P. Bucher, and J. Buffet, Surf. Sci. **127**, 165 (1983).
[54] D. Tomanek, S. Mukherjee, and K. H. Benneman, Phys. Rev. B **28**, 665 (1983).
[55] R. S. Berry, H.-P. Cheng, and J. Rose, High Temp. Sci. **27**, 61 (1989).
[56] G. Wulff, Z. Krist. **34**, 449 (1901).
[57] C. Herring, Phys. Rev. **82**, 87 (1951).
[58] S. Ino, J. Phys. Soc. Jpn. **27**, 941 (1969).
[59] C. Y. Yang, J. Cryst. Growth **47**, 274 (1979).
[60] B. G. Bagley, Nature **209**, 674 (1965).
[61] B. G. Bagley, Nature **225**, 1040 (1970).
[62] S. M. Foiles, M. I. Baskes, and M. S. Daw, Phys. Rev. B **33**, 7983 (1986).
[63] M. S. Daw and M. I. Baskes, Phys. Rev. B **29**, 6443 (1984).
[64] M. I. Baskes, M. Daw, B. Dodson, and S. Foiles, Mater. Res. Soc. Bull. **13**, 28 (1988).
[65] J. B. Adams, S. M. Foiles, and W. G. Wolfer, J. Mater. Res. **4**, 102 (1989).
[66] W. A. Harrison, *Pseudopotentials in the Theory of Metals* (Benjamin, Reading, Mass., 1966).
[67] R. N. Barnett, C. L. Cleveland, and U. Landman, Phys. Rev. Lett. **54**, 1679 (1985).
[68] R. N. Barnett, C. L. Cleveland, and U. Landman, Phys. Rev. Lett. **55**, 2035 (1985).
[69] R. N. Barnett, C. L. Cleveland, and U. Landman, Phys. Rev. B **28**, 1685 (1983).
[70] E. T. Cheng, R. N. Barnett, and U. Landman, Phys. Rev. B **40**, 924 (1989).
[71] E. T. Cheng, R. N. Barnett, and U. Landman, Phys. Rev. B **41**, 439 (1990).
[72] U. Landman, W. D. Luedtke, N. A. Burnham, and R. J. Colton, Science **248**, 454 (1990).
[73] K. W. Jacobson, J. K. Norskov, and M. J. Puska, Phys. Rev. B **35**, 7423 (1987).
[74] J. K. Norskov, Phys. Rev. B **26**, 2875 (1982).
[75] P. Hohenberg and W. Kohn, Phys. Rev. B **136**, 864 (1964).

[76] Assuming fcc structure, no surface relaxation, and only nearest-neighbor bonds.

[77] M. Parrinello and A. Rahman, Phys. Rev. Lett. **45**, 1196 (1980).

[78] Routine *ZXCGR* in the *IMSL Fortran Subroutines for Mathematics and Statistics*, edition 9.2 (IMSL, Inc., Houston, 1984).

[79] Whenever we report properties for extended systems whose energies we have minimized, we use many decimal places. We will want to use such results in macroscopic calculations and compare the results for different applied strains. Under different strains such properties differ by only a small percentage, so we must carry extra figures.

[80] In general, which crystal face will be exposed will depend on which periodic boundary condition is removed as well as the choice of computational cell and the atoms within it, as seen more explicitly in Appendix A.

[81] W. R. Tyson and W. A. Miller, Surf. Sci. **62**, 267 (1977).

[82] J. Q. Broughton and G. H. Gilmer, J. Chem. Phys. **84**, 5741 (1986).

[83] The octahedral site is at the geometric center of the conventional fcc unit cell. It is so called because its six nearest atomic neighbors sit at the vertices of an octahedron.

[84] All perfect cuboctahedra are atom centered.

[85] These model C clusters are the same as the ones used by Raoult *et al.* (Ref. 8). Unfortunately, their description of model C does not produce this set of clusters, but a similar set missing every fourth member of model C.

[86] HKI stands for hexakaiicosahedrons, since they have 26 sides.

[87] A. Mackay, Acta Crystallogr. **15**, 916 (1962).

[88] Interpolation of cuboctahedral or icosahedral energies proceeds in the following way: for a given number of atoms, the cubic formula $N = 1 + (11n + 15n^2 + 10n^3)/3$ for the number of atoms in the cluster is inverted to obtain a nonintegral shell number. The energies of the four nearest clusters of that shape, two smaller and two larger, are used to determine the four coefficients of a cubic equation for energy used in the region between the two nearest such clusters. If we want to extrapolate energies, we simply use the cubic equation in the closest region for which one could be obtained. This method can be tested by omitting a data point, either inside our data range or at its ends, and then checking how well interpolation or extrapolation can reproduce it. Accuracy is better than 1 meV. The use of a cubic equation for interpolation is deliberate. If the surface planes are taken through surface atoms, the shell number of a cuboctahedron or icosahedron is exactly proportional to any of its linear dimensions, including its "radius" r. It is very reasonable to expect the energy of a cuboctahedron or icosahedron to have terms varying as r^3, r^2, and r.

[89] It remains unclear why taking surface planes between atomic layers instead of through them should do better when estimating the overall energies of the clusters examined in this study, and worse when examining relative energetic ordering between clusters. If we focus on relative energy differences between clusters of similar size and for that reason take our energies relative to cuboctahedra, it would appear for the clusters of this study that the best location for a surface plane is just a little outside the plane that passes through its surface's atoms.

[90] The value of 1600 atoms is given in Ref. 8 for the transition to decahedral structures from icosahedra with all vertex atoms removed. No transition size is given for full icosahedra.

[91] The value of 2100 atoms is given in Ref. 8 for the transition, with decahedra disallowed, to single crystal structures and their monotwins from full icosahedra. For icosahedra missing their vertex atoms, which we have not considered here, the value reported in that reference is 2400 atoms.

[92] In the modified Wulff construction, the twinning energy of a twinning plane is divided between the two decahedra that meet at it. Thus the decahedron is treated as containing ten twinning planes, two per tetrahedral unit.